

Tracking the validity of the quasi-static and sub-horizon approximations in modified gravity

J. Bayron Orjuela-Quintana,^{*,1} Savvas Nesseris,^{‡,2}

¹Departamento de Física, Universidad del Valle, Ciudad Universitaria Meléndez, 760032, Cali, Colombia

²Instituto de Física Teórica UAM-CSIC, Universidad Autonóma de Madrid, Cantoblanco, 28049 Madrid, Spain

E-mail: [* john.orjuela@correounivalle.edu.co](mailto:john.orjuela@correounivalle.edu.co), [† savvas.nesseris@csic.es](mailto:savvas.nesseris@csic.es)

Abstract. Within the framework of modified gravity, the quasi-static and sub-horizon approximations are widely used in analyses aiming to identify departures from the concordance model at late-times. Under these approximations, it is generally assumed that time derivatives are subdominant with respect to spatial derivatives given that the relevant physical modes are those well inside the Hubble radius. Here, in the context of the effective fluid approach applied to $f(R)$ theories, we put forward a new parameterization which allows us to obtain analytical expressions for the gravitational potentials, whence for the effective dark energy perturbations. In order to track the validity of the two aforementioned approximations, we compare our results and the standard results found in the literature against full numerical solutions for two well-known toy-models; namely, the designer (f DES) model and the Hu-Sawicki (HS) model. We find that: *i*) the sub-horizon approximation can be safely applied for scales $k \gtrsim 200H_0$, *ii*) in this “safety region”, the quasi-static approximation is a very accurate description of the late-time dynamics even when dark energy significantly contribute to the cosmic budget, *iii*) some relevant terms were neglected in the standard procedure yielding to inaccurate results in some of the dark energy effective fluid quantities; e.g. the sound speed. Instead, our expressions show overall agreement with respect to the full solutions. Therefore, our results indirectly indicate that the effective fluid expressions derived for more general modified gravity theories, such as Horndeski, should be revisited.

¹Corresponding author.

Contents

1	Introduction	1
2	Theoretical Framework	3
2.1	General Setup	3
2.2	Background and Perturbations	3
3	$f(R)$ Theories	4
3.1	Quasi-Static and Sub-Horizon Approximations: Standard Approach	6
4	Tracking the Accuracy of the QSA and the SHA	7
5	Specific $f(R)$ Models	10
5.1	f DES Model	10
5.2	Hu-Sawicki Model	10
6	Numerical Solution of the Evolution Equations	12
6.1	Full Numerical Solution	12
6.2	Comparing Results	13
6.2.1	Gravitational Potentials	14
6.2.2	Dark Energy Perturbations	14
6.2.3	Other Scales	15
7	Impact on Cosmological Observables	16
7.1	The Viscosity parameter	17
7.2	The Matter Power Spectrum	18
8	Conclusions	19
A	Linear Field Equations in $f(R)$	20
B	Dark Energy Perturbations in $f(R)$	20
C	Linear Field Equations in the New Parameterization	20

1 Introduction

The current theoretical paradigm, namely the cosmological constant Λ and cold dark matter (CDM) model (Λ CDM) [1], has started to be challenged by several observations [2–4]. The well-known H_0 tension is now approximately 5σ [5–9], while the S_8 tension is about 2 – 3σ [10–20]. Recently, the inconsistency between the amplitude of the Cosmic Microwave Background (CMB) dipole and the Quasars dipole has exceeded 5σ , setting serious concerns on the cosmological principle [21–24]. These discrepancies and others (see Refs. [25–27]) motivate a further examination of the viability of Λ CDM as the standard cosmological model [28–30], and the exploration of models violating the cosmological principle [31–39].

Generally, the main alternatives to the Λ CDM model imply either the existence of a fluid with negative pressure known as Dark Energy (DE) [40, 41], or covariant modifications to the geometric sector describing gravity, the so-called Modified Gravity (MG) theories [42, 43]. With respect to MG theories, a large portion of the candidate models among these theories are ruled out by observations from, for example, gravitational waves [44, 45], and very precise extra-galactic tests [46–48]. However, there remains some alternatives. Among the still cosmologically viable MG theories, one of the most representative are the so-called $f(R)$ theories [49]. In principle, these theories could be distinguished from the standard cosmological model by their influence in the inhomogeneous Universe since, in general, they introduce modification in several observables, e.g. the growth rate [50]. However, no $f(R)$ model is particularly favored by current growth data [51, 52].

It is fair to say that the distinction between DE and MG is rather academic in a sense, as both scenarios can be treated on equal footing under the Effective Fluid Approach (EFA) [53].¹ Within the EFA, all the modifications to gravity are encompassed in terms of the equation of state w_{DE} , the sound speed $c_{s,\text{DE}}^2$, and the anisotropic stress π_{DE} of an ideal DE fluid. As shown in Refs. [58–60], the application of the Quasi-Static Approximation (QSA) and the Sub-Horizon Approximation (SHA) allows to get analytical expressions for the effective DE perturbations in very general MG theories. One of the advantages of this approach is that these expressions can be easily introduced in Boltzmann solvers, such as CLASS [61], facilitating the computation of cosmological observables; e.g. the linear matter power spectrum or the CMB angular power spectrum.

These approximations also enable us to directly discriminate departures from General Relativity (GR), which could be encoded in, for instance, the effective Newton's constant G_{eff} and the effective lensing parameter Q_{eff} . Albeit they have been extensively used in the literature [62–71], some works claim that the QSA, in particular, can be too aggressive and that relevant dynamical information could be omitted after their application [72, 73]. Therefore, the determination of the accuracy of these approximations is a highly relevant issue to be addressed in order to compare theoretical results with upcoming astrophysical observations.

Bearing in mind the above discussion, we propose to analyze the validity regime in time and scale of the QSA-SHA for modified gravity theories. In order to do so, we parameterize the time evolution of the gravitational potentials, and also parameterize the length scale with respect to the Hubble radius in $f(R)$ theories. This allows us to find analytical expressions for the gravitational potentials, and then expressions for the perturbations of the effective DE fluid. We find that the QSA provides very accurate descriptions of the gravitational potentials. However, we point out some relevant terms that were neglected in some of the effective DE quantities, which can affect the computation of the cosmological observables.

This paper is organized as follows: in Sec. 2, we present the theoretical framework of linear cosmological perturbations around a Friedmann-Lemaître-Robertson-Walker (FLRW) metric. In Sec. 3, the EFA is applied to $f(R)$ theories, and the standard QSA-SHA procedure is used to obtain well-known expressions for the gravitational potentials and the DE perturbations. Then, in Sec. 4, we introduce the new parameterization of the QSA-SHA and write down the dynamics in terms of these parameters. Since these parameters depend on the cosmological model, we introduce some specific $f(R)$ models in Sec. 5. Then, in Sec. 6, we compare the results obtained via the new parameterization, the standard QSA-SHA proce-

¹Another approach which allows to model dark energy and modified gravity in a general framework is the Effective Field Theory (see Refs. [54–57]).

dure, and the full numerical solution when no approximations are used. We give a summary and our conclusions in Sec. 8.

2 Theoretical Framework

2.1 General Setup

In GR, gravitational interactions are characterized by the Einstein-Hilbert action

$$S_{\text{EH}} = \int d^4x \sqrt{-g} \left[\frac{1}{2\kappa} R + \mathcal{L} \right], \quad (2.1)$$

where $\kappa = 8\pi G_N$, G_N is the Newton's constant, g is the determinant of the metric $g_{\mu\nu}$, R is the Ricci scalar, and \mathcal{L} is a Lagrangian for all matter fields. On cosmological scales, the Universe is approximately homogeneous and isotropic [5]. Hence, its geometry can be described by the flat perturbed FLRW metric that in the Newtonian gauge reads

$$ds^2 = -\{1 + 2\Psi(\mathbf{x}, t)\}dt^2 + a(t)^2\{1 + 2\Phi(\mathbf{x}, t)\}\delta_{ij}dx^i dx^j, \quad (2.2)$$

where a is the scale factor, and Ψ and Φ are the gravitational potentials which depend on both the spatial coordinates \mathbf{x} and the cosmic time t . The dynamics is encoded in the Einstein field equations

$$G^\mu_\nu = \kappa T^\mu_\nu, \quad T^\mu_\nu = (\rho + P)u^\mu u_\nu + P\delta^\mu_\nu, \quad (2.3)$$

where G^μ_ν is the Einstein tensor, T^μ_ν is the energy-momentum tensor which is given in terms of the density ρ , the pressure P , and the velocity four-vector $u^\mu = (1 - \Psi, \frac{v^i}{a})$, with² $v^i = a(t)\dot{x}^i$. The components of the energy-momentum tensor are given by

$$T^0_0 = -(\bar{\rho} + \delta\rho), \quad T^0_i = a(t)(\bar{\rho} + \bar{P})ik_iv, \quad T^i_j = (\bar{P} + \delta P)\delta^i_j + \Sigma^i_j, \quad (2.4)$$

where $\bar{\rho}$ and \bar{P} are the background density and pressure, $\delta\rho$ and δP are their respective perturbations, v defined from $v_i \equiv ik_iv$ is the velocity perturbation, k_i is the wave-vector in Fourier space, and Σ^i_j is the anisotropic stress tensor.

2.2 Background and Perturbations

Since we are interested in the late-time cosmological dynamics, we assume that the cosmic fluid is solely composed by pressure-less matter and a dark energy component with equation of state³ $\bar{P}_{\text{DE}} \equiv w_{\text{DE}}\bar{\rho}_{\text{DE}}$, where w_{DE} depends on time in general. This model is known as w CDM, and Λ CDM can be viewed as the particular case when $w_{\text{DE}} = -1$. For the background metric in Eq. (2.2), the unperturbed Einstein field equations (2.3) give rise to the Friedmann equations

$$H^2 = \frac{\kappa}{3}(\bar{\rho}_m + \bar{\rho}_{\text{DE}}), \quad \dot{H} = -\frac{\kappa}{2}[\bar{\rho}_m + \bar{\rho}_{\text{DE}}(1 + w_{\text{DE}})], \quad (2.5)$$

where $H \equiv \dot{a}/a$ is the Hubble parameter. The linearized Einstein equations read

$$\frac{k^2}{a^2}\Phi + 3H(\dot{\Phi} - H\Psi) = \frac{\kappa}{2}(\bar{\rho}_m\delta_m + \bar{\rho}_{\text{DE}}\delta_{\text{DE}}), \quad (2.6)$$

²An over-dot denotes derivative with respect to t .

³In our notation, the subscripts m and DE means that the respective quantity is associated to matter or dark energy. Also note that we have set the speed of light as $c = 1$.

$$k^2 \left(\dot{\Phi} - H \Psi \right) = -\frac{\kappa}{2} a [\bar{\rho}_m \theta_m + \bar{\rho}_{\text{DE}} (1 + w_{\text{DE}}) \theta_{\text{DE}}], \quad (2.7)$$

$$\ddot{\Phi} + H \left(3\dot{\Phi} - \dot{\Psi} \right) - \left(2\dot{H} + 3H^2 \right) \Psi + \frac{k^2}{3a^2} (\Phi + \Psi) = -\frac{\kappa}{2} \delta P_{\text{DE}}, \quad (2.8)$$

$$-\frac{k^2}{a^2} (\Phi + \Psi) = \frac{3\kappa}{2} \bar{\rho}_{\text{DE}} (1 + w_{\text{DE}}) \sigma_{\text{DE}}, \quad (2.9)$$

corresponding to the “time-time”, longitudinal “time-space”, trace “space-space”, and longitudinal trace-less “space-space” parts of the gravitational field equations (2.3), respectively. In the later equations we have define the following quantities: the perturbation over-density or density contrast $\delta \equiv \delta\rho/\bar{\rho}$, the velocity divergence $\theta \equiv ik^i v_i = -k^2 v$, and the scalar anisotropic stress $(\bar{\rho} + \bar{P})\sigma \equiv -(\hat{k}_i \hat{k}_j - \frac{1}{3}\delta_{ij})\Sigma^{ij}$, where $k^2 \equiv k_i k^i$ and $\hat{k}_i \equiv k_i/k$. We have assumed that matter is also pressure-less at first order ($\delta P_m = 0$) and that it has no anisotropic stress ($\sigma_m = 0$).

The conservation of the energy-momentum tensor, namely $\nabla_\mu T^\mu_\nu = 0$, impose the following zero-order continuity equations for matter and DE

$$\dot{\bar{\rho}}_m + 3H\bar{\rho}_m = 0, \quad \dot{\bar{\rho}}_{\text{DE}} + 3H(1 + w_{\text{DE}})\bar{\rho}_{\text{DE}} = 0. \quad (2.10)$$

At linear order we have

$$\delta'_m = -3\Phi' - \frac{V_m}{a^2 H}, \quad (2.11)$$

$$V'_m = -\frac{V_m}{a} + \frac{k^2}{a^2 H} \Psi, \quad (2.12)$$

$$\delta'_{\text{DE}} = -3(1 + w_{\text{DE}})\Phi' - \frac{V_{\text{DE}}}{a^2 H} - \frac{3}{a} (c_{s,\text{DE}}^2 - w_{\text{DE}}) \delta_{\text{DE}}, \quad (2.13)$$

$$V'_{\text{DE}} = -(1 - 3w_{\text{DE}}) \frac{V_{\text{DE}}}{a} + \frac{k^2}{a^2 H} c_{s,\text{DE}}^2 \delta_{\text{DE}} + (1 + w_{\text{DE}}) \frac{k^2}{a^2 H} \Psi - \frac{2}{3} \frac{k^2}{a^2 H} \pi_{\text{DE}}, \quad (2.14)$$

where we have defined the scalar velocity $V \equiv (1 + w)\theta$, the sound speed $c_s^2 \equiv \frac{\delta P}{\delta \rho}$, the anisotropic stress parameter $\pi \equiv \frac{3}{2}(1 + w)\sigma$, and a prime denotes derivative with respect to the scale factor.

In brief, to know the evolution of the large scale structure inhomogeneities of the Universe requires to solve the coupled set of differential equations given by the Einstein equations and the continuity equations, both at background and at linear order. As we will see in the next section, this task can be highly simplified for $f(R)$ theories under some well-motivated assumptions, namely the quasi-static and the sub-horizon approximations.

3 $f(R)$ Theories

In $f(R)$ models, covariant modifications of GR are performed by replacing R in the Einstein-Hilbert action in Eq. (2.1) by a general function $f(R)$ such that

$$S = \int d^4x \sqrt{-g} \left[\frac{1}{2\kappa} f(R) + \mathcal{L} \right]. \quad (3.1)$$

Upon varying this action with respect to the metric $g^{\mu\nu}$, the Einstein equations in Eq. (2.3) are replaced by

$$FG_{\mu\nu} - \frac{1}{2} (f - FR) g_{\mu\nu} + (g_{\mu\nu} \square - \nabla_\mu \nabla_\nu) F = \kappa T_{\mu\nu}, \quad (3.2)$$

where⁴ $F \equiv f_R$. Yet, it is possible to recast Eq. (3.2) to look as the usual Einstein field equations (2.3) using the effective fluid approach. Under this framework, all the modifications to gravity are encoded in a generalized DE fluid which, in the case of $f(R)$ theories, is characterized by the following energy-momentum tensor

$$\kappa T_{\mu\nu}^{(\text{DE})} = (1 - F) G_{\mu\nu} + \frac{1}{2} (f - FR) g_{\mu\nu} - (g_{\mu\nu} \square - \nabla_\mu \nabla_\nu) F. \quad (3.3)$$

Hence, the background equations are given by Eqs. (2.5) replacing the DE density and pressure by

$$\kappa \bar{\rho}_{\text{DE}} = -\frac{f}{2} + 3H^2 (1 + F) + 3F\dot{H} - 3H\dot{F}, \quad (3.4)$$

$$\kappa \bar{P}_{\text{DE}} = \frac{f}{2} - 3H^2 (1 + F) - \dot{H} (2 + F) + 2H\dot{F} + \ddot{F}, \quad (3.5)$$

On the other hand, linear perturbation equations in Eqs. (2.6)-(2.9) are modified as

$$0 = -\kappa \bar{\rho}_m \delta_m + A_1 \dot{\Phi} + A_2 \dot{\Psi} + \left(A_3 + A_4 \frac{k^2}{a^2} \right) \Phi + \left(A_5 + A_6 \frac{k^2}{a^2} \right) \Psi, \quad (3.6)$$

$$0 = -\frac{a\kappa \bar{\rho}_m V_m}{k^2} + C_1 \dot{\Phi} + C_2 \dot{\Psi} + C_3 \Phi + C_4 \Psi, \quad (3.7)$$

$$0 = B_1 \ddot{\Phi} + B_2 \ddot{\Psi} + B_3 \dot{\Phi} + B_4 \dot{\Psi} + B_5 \Phi + B_6 \Psi, \quad (3.8)$$

$$0 = D_1 \ddot{\Phi} + D_2 \dot{\Phi} + D_3 \dot{\Psi} + \left(D_4 + D_5 \frac{k^2}{a^2} \right) \Phi + \left(D_6 + D_7 \frac{k^2}{a^2} \right) \Psi, \quad (3.9)$$

The last equation is obtained from the usual relation

$$0 = F_R(\Phi + \Psi) + F\delta R, \quad (3.10)$$

where δR is the perturbation of the Ricci scalar which in the metric (2.2) reads

$$\delta R = 6\ddot{\Phi} + 24H\dot{\Phi} - 6H\dot{\Psi} + 4\frac{k^2}{a^2}\Phi + \left(2\frac{k^2}{a^2} - 12\dot{H} + 24H^2 \right) \Psi. \quad (3.11)$$

The coefficients A_i , C_i , B_i , and D_i can be found in Appendix A. In the EFA, we can assign to the $f(R)$ theory an effective DE perturbation variable for density, pressure, velocity, and anisotropic stress respectively. They are given by

$$\kappa \delta \rho_{\text{DE}} = W_1 \dot{\Phi} + W_2 \dot{\Psi} + \left(W_3 + W_4 \frac{k^2}{a^2} \right) \Phi + \left(W_5 + W_6 \frac{k^2}{a^2} \right) \Psi, \quad (3.12)$$

$$\kappa \delta P_{\text{DE}} = Y_1 \ddot{\Phi} + Y_2 \ddot{\Psi} + Y_3 \dot{\Phi} + Y_4 \dot{\Psi} + \left(Y_5 + Y_6 \frac{k^2}{a^2} \right) \Phi + \left(Y_7 + Y_8 \frac{k^2}{a^2} \right) \Psi, \quad (3.13)$$

$$\frac{a\kappa \bar{\rho}_{\text{DE}}}{k^2} V_{\text{DE}} = Z_1 \dot{\Phi} + Z_2 \dot{\Psi} + Z_3 \Phi + Z_4 \Psi, \quad (3.14)$$

$$\kappa \bar{\rho}_{\text{DE}} \pi_{\text{DE}} = -\frac{k^2}{a^2} (\Phi + \Psi), \quad (3.15)$$

where the coefficients W_i , Y_i , and Z_i can be found in Appendix B.

⁴We denote derivatives with respect to R by means of an sub-index; e.g. $\frac{df}{dR} \equiv f_R$.

3.1 Quasi-Static and Sub-Horizon Approximations: Standard Approach

The dynamics of DE and matter inhomogeneities in $f(R)$ models can be unveiled if the evolution of the gravitational potentials is known. However, this implies to solve Eqs. (3.6)-(3.9) coupled to the matter perturbations equations in Eqs. (2.11) and (2.12), which in general is a difficult task. As explained in Sec. 1, the application of the Quasi-Static Approximation (QSA) and the Sub-Horizon Approximation (SHA) can greatly simplify the related equations. In the following, we disregard time-derivatives of the potentials and consider that relevant modes for the cosmological dynamics are those well-inside the Hubble radius; i.e. $k \gg aH$. This allows us to neglect terms of the form $H \times$ perturbation in favor of terms of the form $k^2 \times$ perturbation. As an example, applying these approximations to the perturbation of the Ricci scalar in Eq. (3.11) gives

$$\begin{aligned}\delta R &= 6\ddot{\Phi} + 24H\dot{\Phi} - 6H\dot{\Psi} + 4\frac{k^2}{a^2}\Phi + \left(2\frac{k^2}{a^2} - 12\dot{H} + 24H^2\right)\Psi \\ &\stackrel{\text{QSA}}{\approx} 4\frac{k^2}{a^2}\Phi + \left(2\frac{k^2}{a^2} - 12\dot{H} + 24H^2\right)\Psi \\ &\stackrel{\text{SHA}}{\approx} 4\frac{k^2}{a^2}\Phi + 2\frac{k^2}{a^2}\Psi.\end{aligned}$$

Using the QSA-SHA in the linear equations (3.6) and (3.9) we get two algebraic equations for the two potentials, namely

$$0 = -\kappa\bar{\rho}_m\delta_m + A_4\frac{k^2}{a^2}\Phi + A_6\frac{k^2}{a^2}\Psi, \quad (3.16)$$

$$0 = \left(D_4 + D_5\frac{k^2}{a^2}\right)\Phi + \left(D_6 + D_7\frac{k^2}{a^2}\right)\Psi, \quad (3.17)$$

from which we can solve directly for Φ and Ψ in terms of δ_m . The solution is

$$\frac{k^2}{a^2}\Phi = -\frac{\left(D_6 + D_7\frac{k^2}{a^2}\right)\kappa\bar{\rho}_m\delta_m}{(A_6D_5 - A_4D_7)\frac{k^2}{a^2} + (A_6D_4 - A_4D_6)}, \quad (3.18)$$

$$\frac{k^2}{a^2}\Psi = \frac{\left(D_4 + D_5\frac{k^2}{a^2}\right)\kappa\bar{\rho}_m\delta_m}{(A_6D_5 - A_4D_7)\frac{k^2}{a^2} + (A_6D_4 - A_4D_6)}. \quad (3.19)$$

Note that in Eq. (3.17), we do not neglect $D_4\Phi$ and $D_6\Psi$. The reason is that these terms are associated to the mass of the scalaron m_φ , which can be greater than H for some $f(R)$ models [62]. Replacing the coefficients (see Appendix A) in the last relations we get

$$\frac{k^2}{a^2}\Phi = \frac{F - 12F_R(\dot{H} + 2H^2) + 2\frac{k^2}{a^2}F_R}{2F^2 - 12FF_R(\dot{H} + 2H^2) + 6\frac{k^2}{a^2}FF_R}\kappa\bar{\rho}_m\delta_m, \quad (3.20)$$

$$\frac{k^2}{a^2}\Psi = -\frac{F + 4\frac{k^2}{a^2}F_R}{2F^2 - 12FF_R(\dot{H} + 2H^2) + 6\frac{k^2}{a^2}FF_R}\kappa\bar{\rho}_m\delta_m. \quad (3.21)$$

However, when neglecting H and its derivatives, we get the following well-known expressions

$$\frac{k^2}{a^2}\Phi = \frac{F + 2\frac{k^2}{a^2}F_R}{2F^2 + 6\frac{k^2}{a^2}FF_R}\kappa\bar{\rho}_m\delta_m, \quad \frac{k^2}{a^2}\Psi = -\frac{F + 4\frac{k^2}{a^2}F_R}{2F^2 + 6\frac{k^2}{a^2}FF_R}\kappa\bar{\rho}_m\delta_m. \quad (3.22)$$

Applying the same procedure to the DE perturbations in Eqs. (3.12)-(3.15) we get

$$\delta_{\text{DE}} = \frac{(1-F)F + (2-3F)\frac{k^2}{a^2}F_R}{F(F+3\frac{k^2}{a^2}F_R)} \frac{\bar{\rho}_m}{\bar{\rho}_{\text{DE}}} \delta_m, \quad (3.23)$$

$$\frac{\delta P_{\text{DE}}}{\bar{\rho}_{\text{DE}}} = \frac{1}{3F} \frac{2\frac{k^4}{a^4}F_R + 15\frac{k^2}{a^2}F_R\ddot{F} + 3F\ddot{F}}{3\frac{k^2}{a^2}F_R + F} \frac{\bar{\rho}_m}{\bar{\rho}_{\text{DE}}} \delta_m, \quad (3.24)$$

$$V_{\text{DE}} = \frac{a\dot{F}}{2F} \frac{F + 6\frac{k^2}{a^2}F_R}{3\frac{k^2}{a^2}F_R + F} \frac{\bar{\rho}_m}{\bar{\rho}_{\text{DE}}} \delta_m. \quad (3.25)$$

$$\pi_{\text{DE}} = \frac{\frac{k^2}{a^2}F_R}{F^2 + 3\frac{k^2}{a^2}FF_R} \frac{\bar{\rho}_m}{\bar{\rho}_{\text{DE}}} \delta_m \quad (3.26)$$

which are the usual results found in the literature [53, 58–60]. We will refer to the steps performed to obtain the last expressions as the “standard QSA-SHA procedure”, while the relations for the perturbations, namely Eqs. (3.22)–(3.26), will be called as the “standard QSA-SHA results”.

We want to emphasize on one of the key steps in obtaining the above expressions. After replacing the coefficients in Appendices A and B, we also neglected H and its derivatives by assuming that these terms are subdominant in the SHA. Nonetheless, noting that $\dot{F} = F_R\dot{R}$ and $R = 6(\dot{H} + 2H^2)$, if we drop terms proportional to H or its derivatives, we should naively conclude that $\dot{F} \approx 0$, and thus the pressure perturbation and the scalar velocity would take the following form

$$\frac{\delta P_{\text{DE}}}{\bar{\rho}_{\text{DE}}} \approx \frac{1}{3F} \frac{2\frac{k^2}{a^2}F_R}{3\frac{k^2}{a^2}F_R + F} \frac{\bar{\rho}_m}{\bar{\rho}_{\text{DE}}} \delta_m, \quad V_{\text{DE}} \approx 0. \quad (3.27)$$

As shown in several works (see e.g. Refs. [58]), V_{DE} is small but certainly not zero. Indeed, as we will see in the following section, these last expressions correspond to the zero order solution in our new parameterization of the SHA.

4 Tracking the Accuracy of the QSA and the SHA

Following the discussion in the last section, the main assumptions behind the QSA and the SHA are: firstly, that the potentials do not depend on time, and secondly, that $k \gg aH$ allowing to neglect terms with time-derivatives in comparison with terms scaling as k^2 . Then, in order to know the regime where these approximations can be safely applied, we introduce the dimension-less parameters:

$$\varepsilon \equiv \frac{aH}{k}, \quad \delta \equiv \frac{\dot{\varepsilon}}{\varepsilon H}, \quad \xi \equiv \frac{\ddot{\varepsilon}}{\varepsilon H^2}, \quad \chi \equiv \frac{\ddot{\varepsilon}}{\varepsilon H^3}, \quad (4.1)$$

and

$$\varepsilon_\Phi \equiv \frac{\dot{\Phi}}{\Phi H}, \quad \varepsilon_\Psi \equiv \frac{\dot{\Psi}}{\Psi H}, \quad \chi_\Phi \equiv \frac{\dot{\varepsilon}_\Phi}{\varepsilon_\Phi H}, \quad \chi_\Psi \equiv \frac{\dot{\varepsilon}_\Psi}{\varepsilon_\Psi H}. \quad (4.2)$$

Hence, $k \gg aH$ is translated to $\varepsilon \ll 1$, and $\dot{\Phi} \sim \dot{\Psi} \approx 0$ is translated to $\varepsilon_\Phi \sim \varepsilon_\Psi \ll 1$. We refer to the parameters in Eqs. (4.1) and (4.2) as “SHA parameters” and “QSA parameters”, respectively.⁵

⁵We would like to mention that the QSA parameters are inspired by the slow-roll dynamics utilized in the background analysis of inflationary models, while the SHA parameters were also introduced in e.g. Ref. [72].

We want to comment on some previous considerations before implementing the parameterization into the equations in Sec. 3 describing $f(R)$ theories. First of all, in order to track all the terms proportional to H or its derivatives, we replace time derivatives of F in favor of H ; i.e.

$$\dot{F} = 6F_R(\ddot{H} + 4H\dot{H}), \quad \ddot{F} = 6F_R(\ddot{H} + 4H\ddot{H} + 4\dot{H}^2) + 36F_{RR}(\ddot{H} + 4H\dot{H})^2. \quad (4.3)$$

In addition, apart of the parameter ε , all the other SHA parameters are not necessarily small. For example, during matter domination we have $H = H_0\sqrt{\Omega_{m0}}a^{-3/2}$ and

$$\delta = -1/2, \quad \xi = 1, \quad \chi = -7/2, \quad (\text{in matter domination}) \quad (4.4)$$

where Ω_{m0} is the matter density parameter today, and H_0 is the Hubble constant.

Re-writing Eqs. (3.6) and (3.9) using the new parameters, we obtain the following two “algebraic” equations to solve for Φ and Ψ

$$0 = -\kappa\bar{\rho}_m\delta_m + \mathcal{A}_1\frac{k^2}{a^2}\Phi + \mathcal{A}_2\frac{k^2\varepsilon^2}{a^2}\Phi + \mathcal{A}_3\frac{k^4\varepsilon^4}{a^4}\Phi + \mathcal{A}_4\frac{k^2}{a^2}\Psi + \mathcal{A}_5\frac{k^2\varepsilon^2}{a^2}\Psi + \mathcal{A}_6\frac{k^4\varepsilon^4}{a^4}\Psi, \quad (4.5)$$

$$0 = \left(\mathcal{D}_1 + \mathcal{D}_2\frac{k^2}{a^2}\right)\Phi + \mathcal{D}_3\frac{k^2\varepsilon^2}{a^2}\Phi + \left(\mathcal{D}_4 + \mathcal{D}_5\frac{k^2}{a^2}\right)\Psi + \mathcal{D}_6\frac{k^2\varepsilon^2}{a^2}\Psi, \quad (4.6)$$

where the coefficients \mathcal{A}_i and \mathcal{D}_i are found in Appendix C. Note that we wrote the above equations factorizing in terms of ε in order to facilitate the measurement of the relevance of each term. Now, solving for Φ and Ψ , expanding in powers of ε up to second order, replacing the coefficients \mathcal{A}_i and \mathcal{D}_i , and considering only linear terms in the QSA parameters we get

$$\frac{k^2}{a^2}\Phi = \frac{F + 2\frac{k^2}{a^2}F_R}{2F^2 + 6\frac{k^2}{a^2}FF_R}\kappa\bar{\rho}_m\delta_m + \frac{3\kappa\bar{\rho}_m\delta_m\varepsilon^2}{4F\left(F + 3\frac{k^2}{a^2}F_R\right)^2}\left\{F^2(2 + \varepsilon_\Phi + \varepsilon_\Psi) + 2\frac{k^2}{a^2}FF_R[\delta(1 + \varepsilon_\Phi) + 4(2 + \varepsilon_\Psi) + 5\varepsilon_\Phi] + 4\frac{k^4}{a^4}F_R^2[\delta(3 + \varepsilon_\Phi) + 4(2 + \varepsilon_\Psi) + 4\varepsilon_\Phi]\right\}, \quad (4.7)$$

$$\frac{k^2}{a^2}\Psi = -\frac{F + 4\frac{k^2}{a^2}F_R}{2F^2 + 6\frac{k^2}{a^2}FF_R}\kappa\bar{\rho}_m\delta_m + \frac{3\kappa\bar{\rho}_m\delta_m\varepsilon^2}{4F\left(F + 3\frac{k^2}{a^2}F_R\right)^2}\left\{F^2(2 + \varepsilon_\Phi + \varepsilon_\Psi) - 2\frac{k^2}{a^2}FF_R[\delta(3 + \varepsilon_\Phi) - 3(2 + \varepsilon_\Psi)] - 4\frac{k^4}{a^4}F_R^2[\delta(6 + \varepsilon_\Phi) - 2(2 + \varepsilon_\Psi) + \varepsilon_\Phi]\right\}. \quad (4.8)$$

We recognize the standard expressions for the potentials [see Eq. (3.22)] in the first term on the right-hand side of the last expressions. Hence, we can identify the standard results for the potentials as the solution for the *deepest* modes in the Hubble radius or, equivalently, the smallest scales where $\varepsilon \sim 0$.

Indeed, equations (4.5) and (4.6) are not “algebraic” equations for Φ and Ψ , since the QSA parameters ε_Φ and ε_Ψ depends on the dynamics of the potentials. Therefore, Eqs. (4.7) and (4.8) are coupled differential equations for Φ and Ψ . For simplicity, we avoid this problem by working in the zero order expansion of the QSA parameters; i.e. we will assume that $\varepsilon_\Phi = \varepsilon_\Psi = 0$. However, as we will see, these approximations; namely zero order in QSA parameters and second order terms in SHA parameters, are sufficiently accurate

when compare with full numerical results for large modes. The resulting expressions are

$$\begin{aligned} \frac{k^2}{a^2}\Phi &= \frac{F + 2\frac{k^2}{a^2}F_R}{2F^2 + 6\frac{k^2}{a^2}FF_R}\kappa\bar{\rho}_m\delta_m \\ &+ \frac{3\kappa\bar{\rho}_m\delta_m\varepsilon^2}{2F\left(F + 3\frac{k^2}{a^2}F_R\right)^2}\left\{F^2 + \frac{k^2}{a^2}(\delta + 8)FF_R + 2\frac{k^4}{a^4}(3\delta + 8)F_R^2\right\}, \end{aligned} \quad (4.9)$$

$$\begin{aligned} \frac{k^2}{a^2}\Psi &= -\frac{F + 4\frac{k^2}{a^2}F_R}{2F^2 + 6\frac{k^2}{a^2}FF_R}\kappa\bar{\rho}_m\delta_m \\ &+ \frac{3\kappa\bar{\rho}_m\delta_m\varepsilon^2}{2F\left(F + 3\frac{k^2}{a^2}F_R\right)^2}\left\{F^2 - \frac{k^2}{a^2}(3\delta - 6)FF_R - 2\frac{k^4}{a^4}(6\delta - 4)F_R^2\right\}. \end{aligned} \quad (4.10)$$

Now, applying the new parameterization to the DE perturbations quantities in Eqs. (3.12)-(3.15), and then inserting these potentials we get:

$$\begin{aligned} \delta_{\text{DE}} &= \frac{(1 - F)F + \frac{k^2}{a^2}(2 - 3F)F_R}{F(F + 3\frac{k^2}{a^2}F_R)}\frac{\bar{\rho}_m}{\bar{\rho}_{\text{DE}}}\delta_m \\ &- \frac{3\frac{k^2}{a^2}F_R\varepsilon^2}{F\left(F + 3\frac{k^2}{a^2}F_R\right)^2}\left\{(\delta + 1)F + 2\frac{k^2}{a^2}(3\delta + 2)F_R\right\}\frac{\bar{\rho}_m}{\bar{\rho}_{\text{DE}}}\delta_m, \end{aligned} \quad (4.11)$$

$$\begin{aligned} \frac{\delta P_{\text{DE}}}{\bar{\rho}_{\text{DE}}} &= \frac{1}{3F}\frac{2\frac{k^2}{a^2}F_R}{3\frac{k^2}{a^2}F_R + F}\frac{\bar{\rho}_m}{\bar{\rho}_{\text{DE}}}\delta_m + \frac{3\frac{\bar{\rho}_m}{\bar{\rho}_{\text{DE}}}\delta_m\varepsilon^2}{F\left(F + 3\frac{k^2}{a^2}F_R\right)^2}\left\{F^2(F - 1)(1 + 2\delta) \right. \\ &\left. + \frac{k^2}{a^2}(5F - 10\delta + 13F\delta - 5)FF_R + 2\frac{k^4}{a^4}(6F - 6\delta + 21F\delta - 4)F_R^2\right\}, \end{aligned} \quad (4.12)$$

$$V_{\text{DE}} = \frac{a}{F\left(F + 3\frac{k^2}{a^2}F_R\right)}\left\{F(F - 1) + \frac{k^2}{a^2}(3F - 4)F_R\right\}\frac{\bar{\rho}_m}{\bar{\rho}_{\text{DE}}}\delta_m\frac{k}{a}\varepsilon, \quad (4.13)$$

$$\pi_{\text{DE}} = \frac{\frac{k^2}{a^2}F_R}{F^2 + 3\frac{k^2}{a^2}FF_R}\frac{\bar{\rho}_m}{\bar{\rho}_{\text{DE}}}\delta_m + \frac{3F_R\frac{\bar{\rho}_m}{\bar{\rho}_{\text{DE}}}\delta_m\frac{k^2}{a^2}\varepsilon^2}{F\left(F + 3\frac{k^2}{a^2}F_R\right)^2}\left\{F(1 + 2\delta) + \frac{k^2}{a^2}F_R(4 + 9\delta)\right\}. \quad (4.14)$$

From the last expressions, we can unravel similarities and differences between the standard QSA-SHA results in Eqs. (3.22)-(3.26) and our expressions in Eqs. (4.9)-(4.14). For instance, we see that the standard δ_{DE} in Eq. (3.23) corresponds to the zero order contribution in Eq. (4.11). In the new parameterization δP_{DE} has contributions to second order in ε , while V_{DE} is prominently a first order quantity in the ε -expansion. Now, bearing in mind that

$$\dot{F} = 6\frac{k^3}{a^3}(\delta + \xi - 2)F_R\varepsilon^3, \quad (4.15)$$

$$\ddot{F} = 6\frac{k^4}{a^4}(\delta^2 - 8\delta + \chi + 6)F_R\varepsilon^4 + 36\frac{k^6}{a^6}(\delta + \xi - 2)F_R\varepsilon^6, \quad (4.16)$$

we note that, in the new SHA parameterization, the standard δP_{DE} in Eq. (3.24) corresponds to a zero order quantity plus fourth and sixth order corrections, while the standard V_{DE} in Eq. (3.25) is entirely a third order quantity.

In order to determine the relevance of the terms neglected in the standard QSA-SHA procedure, we have to track the evolution of the SHA parameters which depend on H and its derivatives; i.e. they depend on the specific cosmological model. In the following section we will study the behaviour of these parameters in the context of two well-known $f(R)$ models: the f DES designer model [74, 75], and the Hu-Sawicki model [76].

5 Specific $f(R)$ Models

5.1 f DES Model

As shown in Refs. [77, 78], $f(R)$ models admit solutions which can be “designed” to reproduce any desirable expansion history. In particular, it is possible to find an $f(R)$ model matching the Λ CDM background but having deviations at the perturbations level. The Lagrangian of this designer model, f DES hereafter, reads [74]

$$f(R) = R - 2\Lambda + \alpha H_0^2 \left(\frac{\Lambda}{R - 3\Lambda} \right)^{c_0} {}_2F_1 \left(c_0, \frac{3}{2} + c_0, \frac{13}{6} + 2c_0, \frac{\Lambda}{R - 3\Lambda} \right), \quad (5.1)$$

where $c_0 \equiv (\sqrt{73} - 7)/12$, α is a dimensionless constant, and ${}_2F_1$ denotes the hypergeometric function. Since the background is the same as in Λ CDM, from Eqs. (3.4) and (3.5) we have

$$H^2 = H_0^2 (\Omega_{m0}a^{-3} + \Omega_{\Lambda0}), \quad \bar{\rho}_{\text{DE}} = -\bar{P}_{\text{DE}} = 3H_0^2\Omega_{\Lambda0}, \quad (5.2)$$

where $\Omega_m \equiv \Omega_{m0}a^{-3}$ and $\Omega_{\Lambda0}$ is the DE density parameter today. The α parameter can be estimated following the prescription that viable $f(R)$ models require

$$f_{R0} \equiv F(a = 1) - 1 \ll 1. \quad (5.3)$$

A typical value is $f_{R0} \sim -10^{-4}$ (see, for instance, Ref. [50]) which translates to $\alpha \approx 0.00107$.

5.2 Hu-Sawicki Model

The Hu-Sawicki (HS) model is a well-known model constructed in such a way that observational tests, such as solar system tests, can be surpassed. Its Lagrangian is given by [76]

$$f(R) = R - m^2 \frac{c_1(R/m^2)^n}{1 + c_2(R/m^2)^n}, \quad (5.4)$$

where m , c_1 , c_2 , and n are dimensionless constant. Through algebraic manipulation, it is possible to re-write the last function as [79]

$$f(R) = R - \frac{2\Lambda}{1 + \left(\frac{b\Lambda}{R}\right)^n}, \quad \Lambda = \frac{m^2 c_1}{2c_2}, \quad b = \frac{2c_2^{1-1/n}}{c_1}. \quad (5.5)$$

Therefore, the background evolution in the HS model can be similar to Λ CDM depending on b and n . Usually n takes on positive integer values. Here, we choose $n = 1$. Assuming $f_{R0} = -10^{-4}$, we estimate $b \approx 0.000989557$.

In order to characterize the background evolution of the HS model, in general we would have to solve the Friedmann equations (2.5) and the continuity equations (2.10). However, we can evade this issue by using the following analytical approximation to the Hubble parameter [79]

$$H_{\text{HS}}(a)^2 = H_{\Lambda}(a)^2 + b \delta H_1(a)^2 + \mathcal{O}(b^2), \quad (5.6)$$

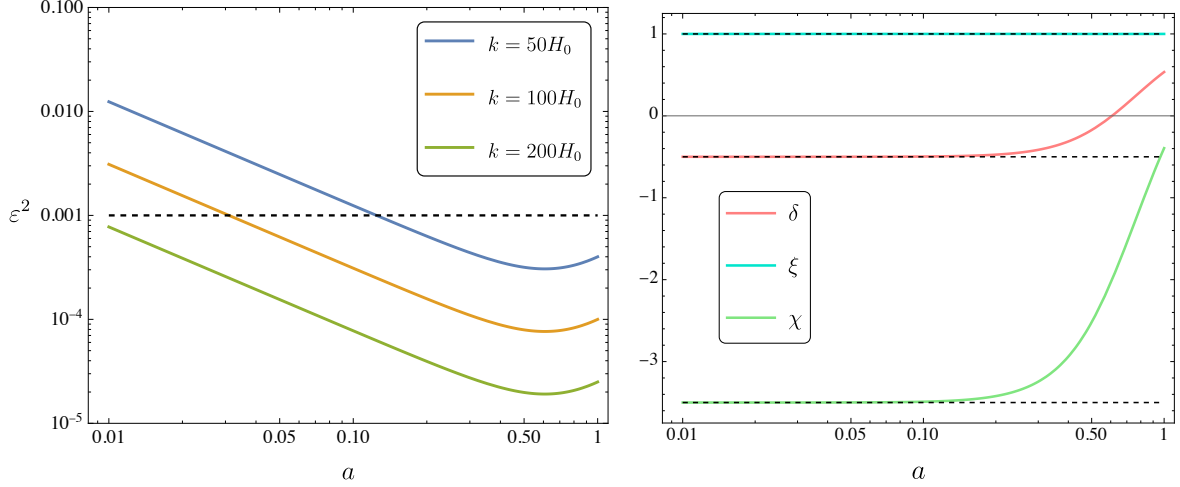


Figure 1. Left: Evolution of the ε parameter in the HS model for three values of k . We can see that $\varepsilon^2 \lesssim 10^{-3}$ during the whole matter dominated epoch until present days for scales $k \gtrsim 200H_0$. Right: Evolution of the SHA parameters δ , ξ , and χ in the HS model. Note that they behave as constants during the matter dominated epoch as expected from Eqs. (4.4) (see the dashed black lines), with a raising at late-times when the contribution of DE becomes more relevant.

where the function $\delta H_1(a)$ is given in the Appendix of Ref. [79] and H_Λ is the Hubble parameter for the Λ CDM model. Overall, Eq. (5.6) is accurate to better than $\sim 10^{-5}\%$, for our choice of the parameter b .

Having the functional forms of H ; Eqs. (5.2) and (5.6) for the f DES and HS models respectively, we can follow the evolution of the SHA parameters defined in Eq. (4.1). However, as noted in Eqs. (5.2) and (5.6), the HS can be regarded as a small deviation from the Λ CDM model for b small enough. We verified that indeed the evolution of the SHA parameters in both models are essentially indistinguishable for the values of α and b we chose. Then, to keep our presentation simple, in Fig. 1 we only plot the evolution of the SHA parameters for the HS model. In the left-panel of this figure, we see that ε^2 can be safely considered as “small” (i.e. $\varepsilon^2 \lesssim 10^{-3}$) for modes $k \gtrsim 200H_0$. In the right panel we see that at earlier times the other SHA parameters behave as expected during the matter dominated epoch [see Eq. (4.4)] and grow when DE plays a more relevant role in the cosmic budget. Therefore, we say that the “safety region” where the SHA can be applied corresponds to the scales $200H_0 \lesssim k \lesssim 600H_0$ which translates to $0.01 h \text{ Mpc}^{-1} \lesssim k \lesssim 0.2 h \text{ Mpc}^{-1}$. Note that the upper bound comes from the fact that this is the maximum comoving wave number associated with the galaxy power spectrum without entering the non-linear regime [70, 80].

We would like to point out that the f DES model and the HS model have a background evolution either identical or similar to that of Λ CDM where in fact the potentials are constant during matter domination, and that $f(R)$ models with different background evolution could yield to different results, in principle. Nonetheless, as clarified in Ref. [81], $f(R)$ models with expansion histories similar to that of Λ CDM are cosmologically viable, while more generic models have in general to meet a number of requirements, making the model-building process more contrived [82].

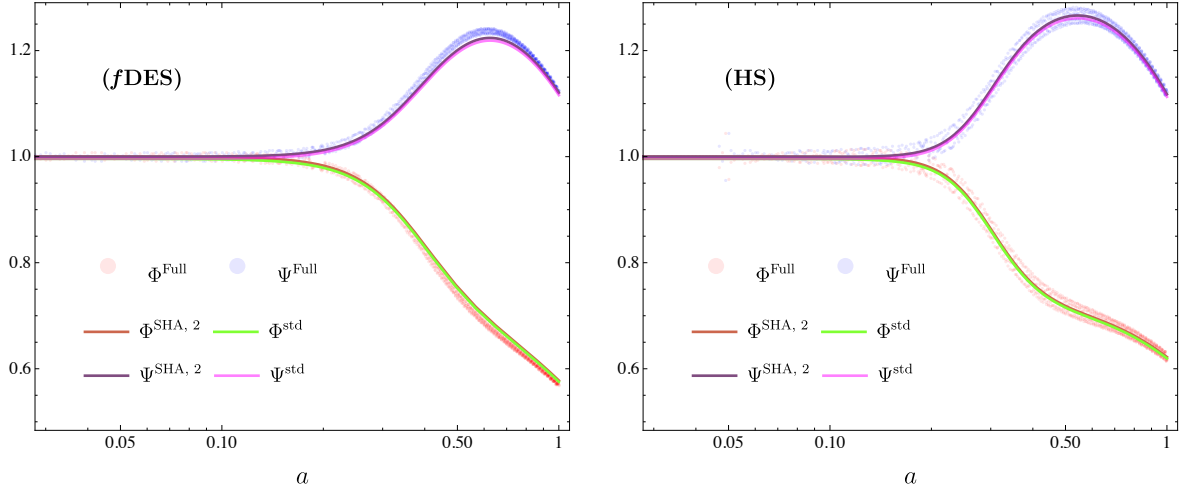


Figure 2. Comparison of the potentials Φ and Ψ obtained from the full numerical solution, from the standard QSA-SHA procedure, and from our new approach. Left panel corresponds to the results for the *fDES* model, while the right panel corresponds to the results for the *HS* model. For the plots we used $k = 300H_0$.

6 Numerical Solution of the Evolution Equations

In this section we numerically solve the equations for matter perturbations in Eqs. (2.11) and (2.12) assuming that Φ and Ψ are given by: *i*) the standard QSA and SHA expressions in Eqs. (3.22), and *ii*) the new parameterized expressions in Eqs. (4.9) and (4.10) where QSA parameters were neglected. Then, we use these solutions to track the evolution of the DE perturbations given by the standard procedure in Eqs. (3.23) and (3.25), and the second order SHA expressions in Eqs. (4.11)-(4.13). We also contrast these results with the full numerical solutions.

6.1 Full Numerical Solution

It is desirable to solve the full set of linear equations in Eqs. (3.6)-(3.9) complemented with the continuity equations in Eqs. (2.11) and (2.12). However, this set of equations is highly unstable, and typical numerical methods do not yield to reliable results. In Ref. [50], this problem was solved by rendering the perturbation equations in a more treatable numerical way which we describe in the following.

Multiplying the “Time-Space” equation (3.7) by $-3H$ and using the “Time-Time” equation (3.6) we get the following Poisson-like equation

$$\frac{k^2}{a^2}(\Phi - \Psi)F = \kappa\bar{\rho}_m\Delta_m - 3\dot{F}\dot{\Phi} - 3F\dot{H}\Phi + (3H\dot{F} - 3F\dot{H})\Psi, \quad (6.1)$$

where we have defined the matter comoving density perturbation

$$\Delta_m = \delta_m + \frac{3aHV_m}{k^2}. \quad (6.2)$$

Now, we define the variables

$$\Phi_+ = \frac{1}{2}(\Phi - \Psi), \quad \zeta = -F(\Phi + \Psi). \quad (6.3)$$

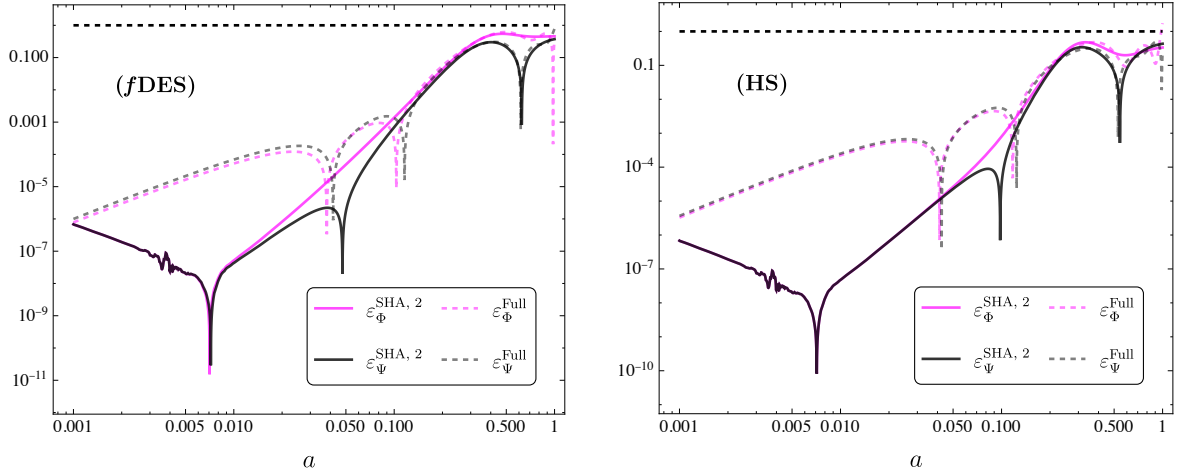


Figure 3. Evolution of the QSA parameters in Eqs. (4.2). For both models (*f*DES on the left panel and HS on the right panel), these parameters are small during the matter dominated epoch and significantly increase around the matter-DE transition.

The evolution equations for these new variables can be obtained from the “Time-Space” equation (3.7) and the Poisson-like equation (6.1). We get

$$\Phi'_{+} = -\frac{a\kappa\bar{\rho}_m V_m}{2FHk^2} - \left(1 + \frac{F'}{2F}\right)\Phi_{+} - \frac{3F'}{4F^2}\zeta, \quad (6.4)$$

$$\zeta' = -\frac{2\kappa\bar{\rho}_m \Delta_m}{3H^2} \frac{F}{F'} + \left(1 + \frac{F'}{F} - 2\frac{F'}{F} \frac{H'}{H}\right)\zeta + 2F\Phi'_{+} + 2F\left(1 + \frac{2}{3}\frac{k^2}{a^2 H^2} \frac{F^2}{F'}\right)\Phi_{+}, \quad (6.5)$$

where a quote ' means derivative with respect to the number of *e*-folds, which is related to the time-derivative by $dN \equiv Hdt$. These equations are complemented with the equations for V_m and δ_m in Eqs. (2.12) and (2.11), having in mind that the relation between scale factor-derivatives and *e*-folds-derivatives is $da \equiv adN$. We assume that there are no deviations from GR at early times, then the initial conditions are

$$\Phi_{+,i} = 1, \quad \zeta_i = 0, \quad V_{m,i} = -\frac{2}{3}\frac{k^2}{a_i H_i} \Phi_{+,i}, \quad \Delta_{m,i} = \frac{2k^2}{3a_i^2 H_i^2} \Phi_{+,i}, \quad (6.6)$$

where the expressions for $V_{m,i}$ and $\Delta_{m,i}$ correspond to the simplification of the “Time-Space” equation (3.7) and the Poisson equation (6.1) in matter dominance; i.e., taking $H^2 = H_0^2 \Omega_{m0} a^{-3}$, and assuming that early modifications to GR are negligible. The overall factor δ_i is set to unity, and we choose $a_i = 10^{-3}$, ensuring initial conditions well within the matter epoch, right after decoupling.

6.2 Comparing Results

In this section, we compare the full numerical solutions, which are obtained using the approach described in the last section, the standard QSA-SHA results (see Sec. 3), and the results from our new parameterization described in Sec. 4, for the two models considered; namely, the *f*DES model and the HS model.

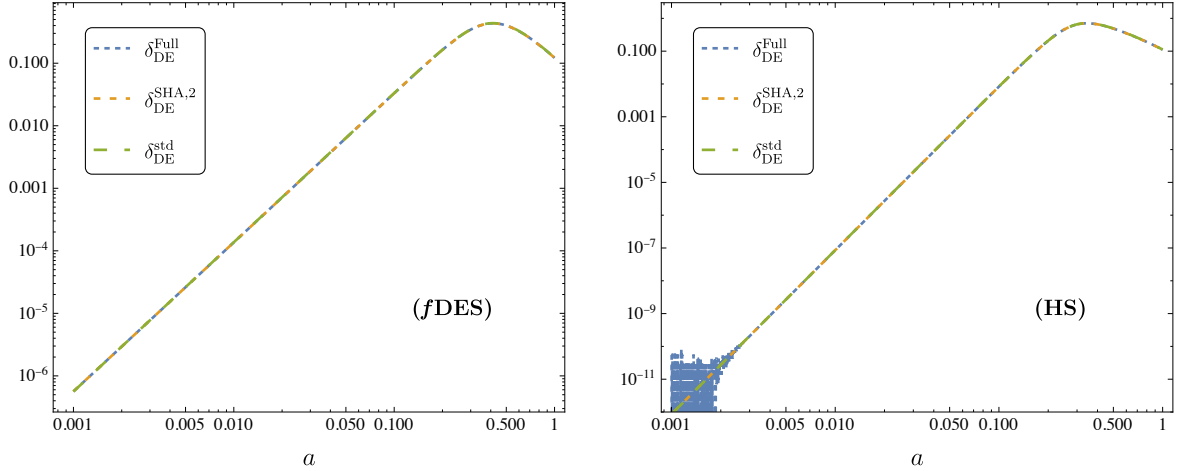


Figure 4. Comparison of the DE contrast obtained from full numerical solution, the standard QSA-SHA approach, and our new parameterization. For both models (*f*DES on the left panel and HS on the right panel), the agreement with the full solution is excellent.

6.2.1 Gravitational Potentials

In order to solve the evolution equations for δ_m and V_m in Eqs. (2.11) and (2.12), we replace the analytic expressions for the potentials Φ and Ψ from either the standard procedure in Eqs. (3.22) or our new expressions in Eqs. (4.9) and (4.10), using the initial conditions [83]:

$$\delta_{m,i} = \delta_i a_i \left(1 + 3 \frac{a_i^2 H^2(a_i)}{k^2} \right), \quad V_{m,i} = -\delta_i H_0 \Omega_{m0} a_i^{1/2}. \quad (6.7)$$

Then, knowing δ_m it is possible to track the evolution of the potentials and, consequently, of the DE perturbations.

As it can be seen in Fig. 2, the full solutions for the potentials for the two models undergo very rapid oscillations with small amplitudes; i.e. they remain well-behaved. This oscillatory behaviour was also pointed out in Refs. [50, 84], where it was attributed to the evolution of δR , this being a generic feature of $f(R)$ models. In both plots, left-panel for the *f*DES model and right panel for the HS model, we can see that the standard QSA-SHA procedure and our new approach give accurate approximations to the full numerical solutions.

From the results for the potentials, it is possible to compute the QSA parameters ε_Φ and ε_Ψ in order to determine the time and scale validity regimes of the QSA; as we did for the SHA in Sec. 5. As depicted in Fig. 3, these parameters are very small ($\lesssim 10^{-3}$) during the whole matter dominated epoch, with a significant increasing at later times. However, they do not reach unity even at present days when $a = 1$. Therefore, we can conclude that in the case of $f(R)$ models under consideration, the assumption that the contributions of the time-derivatives of the potentials to the cosmological dynamics are subdominant can be safely applied for the scales when the SHA is also applicable.

6.2.2 Dark Energy Perturbations

As shown in Fig. 2, the analytical approximations to the potentials are indeed accurate and there is no appreciable differences between the potentials given by the standard QSA-SHA procedure and our approach. Hence, we can compute the full DE perturbations in Eqs. (3.12)-(3.15) using the potentials in Eqs. (4.9) and (4.10), or, equivalently, the standard expressions

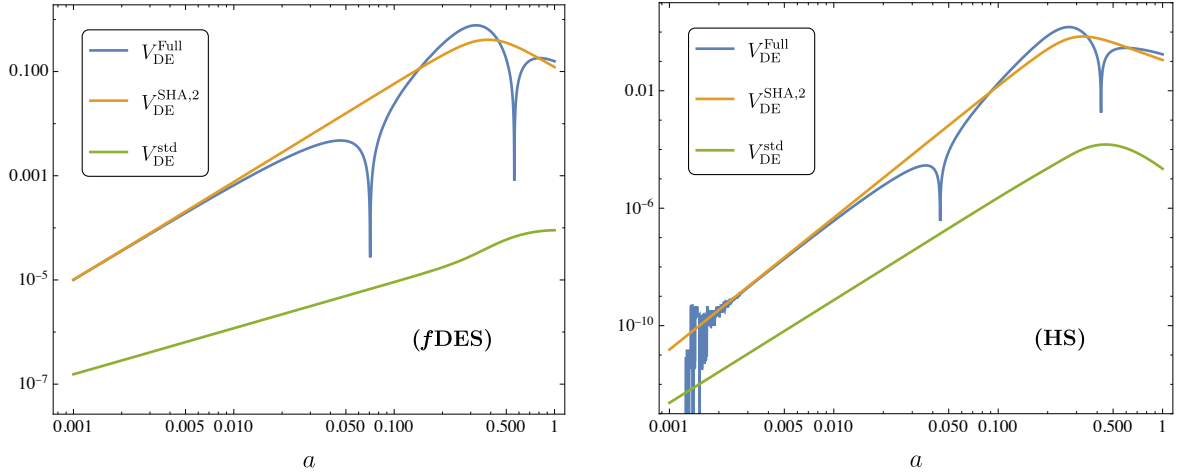


Figure 5. Comparison of the DE scalar velocity obtained from full numerical solution, the standard QSA-SHA procedure, and our new parameterization. For both models (*f*DES on the left panel and HS on the right panel), we see that our expressions show overall agreement with the full V_{DE} , while the standard result is far smaller. This is due to $V_{\text{DE}}^{\text{std}}$ is a third order expression in the new SHA parameterization.

for the potentials in Eqs. (3.22). In Fig. 4, we compare the results for the DE contrast δ_{DE} , where it can be seen that the analytical approximations are in perfect agreement with the full results. However, as expected from the discussion in Sec. 3, there are significant differences between the DE scalar velocity given by the standard approach in Eq. (3.25) and our result at second order in SHA parameters in Eq. (4.13). In Fig. 5, we note that V_{DE} given by the standard QSA-SHA procedure is far smaller than the full V_{DE} , while our second order expression shows overall agreement for both models. It is possible to track the origin of this disagreement. Note that our expression for V_{DE} is a first order expression in the ε -expansion, however, if we use our parameterization in the standard V_{DE} given in Eq. (3.25) we get

$$V_{\text{DE}}^{\text{std}} = \frac{3aF_R}{F} \frac{F + 6\frac{k^2}{a^2}F_R}{F + 3\frac{k^2}{a^2}F_R} (\delta + \xi - 2) \kappa \bar{\rho}_m \delta_m \frac{k^3}{a^3} \varepsilon^3, \quad (6.8)$$

which clearly is a third order expression in the new SHA parameterization.

We verified that a similar problem arises in the case of the pressure perturbation; i.e. it is far smaller than the full solution. The impact of this difference can be seen in the evolution of the sound speed $c_{s,\text{DE}}^2 \equiv \delta P_{\text{DE}}/\delta \rho_{\text{DE}}$. In Fig. 6, it can be noted that the standard result for c_s^2 does not agree with the expected result. However, note that our second order expression remarkably agrees in the case of the *f*DES model with some deviations in the HS model. In $f(R)$ theories, usually the sound speed is negative but the effective sound-speed that also takes into account the DE anisotropic stress is always positive [85].

6.2.3 Other Scales

In order to test the ‘‘safety region’’ where the QSA and the SHA are applicable; namely $k \gtrsim 200H_0$, we compare the potentials obtained from the full solution considering $k = 100H_0$, and their corresponding results from the standard QSA-SHA procedure and our new approach. In the right panel Fig. 7, we see that in the case of the HS model, our zero order

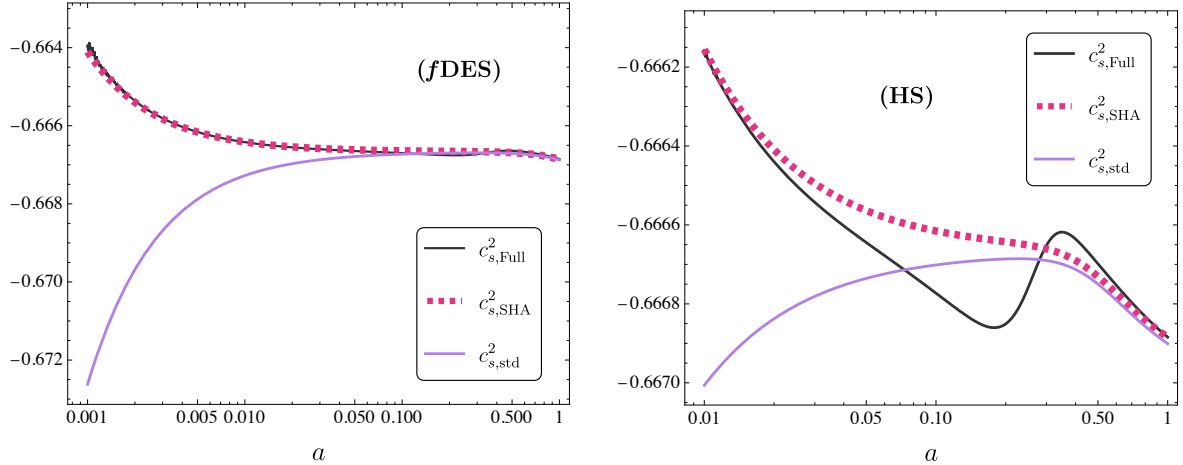


Figure 6. Comparison of the DE sound speed obtained from full numerical solution, the standard QSA-SHA approach, and our new parameterization. For both models (*fDES* on the left panel and *HS* on the right panel), we see that our expressions show overall agreement, excellent for the *fDES* model, with the full c_s^2 , while the standard result has large differences. This is due to $\delta P_{\text{DE}}^{\text{std}}$ is a fourth order expression in the new SHA parameterization.

expansion in QSA parameters and second order expansion in SHA parameters expressions still provides fairly accurate descriptions of the potentials, while the potentials obtained from the standard procedure have an offset diminishing the accuracy of these expressions. This offset in the standard QSA-SHA expressions is also present in the *fDES* model, as it can be seen in the left panel of Fig. 7. Nonetheless, our new expressions also show deviations from the full solutions in this case. This indicates that both methods are not as accurate for $k = 100H_0$ as they are for $k = 300H_0$, as can be seen in Fig. 2, and that the QSA parameters cannot be neglected anymore. As a final remark, we would like to mention that the “safety region” for the applicability of the QSA and the SHA; namely $200H_0 \lesssim k \lesssim 600H_0$, is rather an estimation and not a general statement. The effectiveness of these approximations depends on the specific cosmological model and in this work we only studied models whose background are similar or equal to Λ CDM. However, we recall that $f(R)$ models with a very different background evolution in comparison to Λ CDM are tightly constrained by several tests [50, 81, 82].

7 Impact on Cosmological Observables

As we saw in the last section, some relevant terms are neglected in the DE perturbations when the standard QSA-SHA procedure is applied. So that, drastic modifications are taken into account for some quantities in our approach; e.g. the scalar velocity V_{DE} is raised by roughly three orders of magnitude (see Fig. 5), while some other quantities get minor corrections; such as the sound speed (see Fig. 6). Therefore, it is of great interest to measure the influence of these changes on cosmological observables or parameters used in forecasts. In particular, we will analyze the impact of DE perturbations on: *i*) the viscosity parameter which can be important in weak lensing experiments [86], and *ii*) the matter power spectrum using the **EFCLASS** branch [58] of the Boltzmann solver **CLASS** [61].

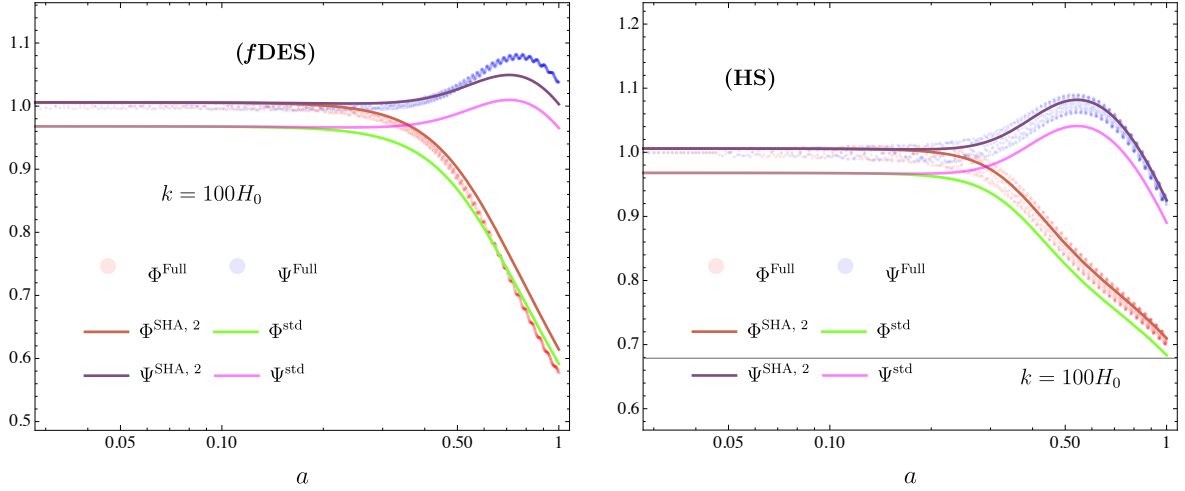


Figure 7. Comparison of the potentials for the f DES model (left panel) and the HS model (right panel) considering a value for k which is out of the “safety region”; i.e. $k < 200H_0$. We see that the standard procedure provides less accurate results in contrast with the results from our approach, which is fairly acceptable for the HS model. However, in the case of the f DES model, results are not as accurate as in Fig. 2.

7.1 The Viscosity parameter

In the Λ CDM model, it is well known that the potentials are related by $\Phi = -\Psi$. As it can be seen in Eq. (3.10), this is not the case in $f(R)$, since this difference can be related to the anisotropic stress as shown in Eq. (3.15). Therefore, a detection of a non-zero anisotropic stress could favored MG theories over single-scalar field models which in general predicts a vanished π_{DE} [85, 87, 88]. The effect of the anisotropic stress can be modelled by introducing a viscosity parameter that appears in the right hand-side of an effective DE anisotropic stress Boltzmann equation of the form [89]:

$$\dot{\sigma} + 3\mathcal{H}\frac{c_a^2}{w}\sigma = \frac{8}{3}\frac{c_{\text{vis}}^2}{(1+w)^2}V_{\text{DE}}, \quad (7.1)$$

where $c_a^2 = w - \frac{\dot{w}}{3\mathcal{H}(1+w)} = w - \frac{aw'}{3(1+w)}$ is the adiabatic sound speed and dots are conformal time derivatives. This can be inverted to solve for the viscosity parameter

$$c_{\text{vis}}^2 = \frac{aH(1+w_{\text{DE}})}{4wV_{\text{DE}}} \left[3c_{a,\text{DE}}^2(1+w_{\text{DE}})\pi_{\text{DE}} + w(a\pi'_{\text{DE}} - 3w\pi_{\text{DE}}) \right], \quad (7.2)$$

which is a function of the scale factor [58, 86, 89]. From the last equation, it is clear that a large modification to V_{DE} could strongly impact the evolution of the viscosity parameter. Indeed, as it can be seen in the left panel of Fig. 8, the viscosity parameter for the HS model in the standard procedure grows at early times reaching values greater than 1 by the end of the matter epoch. Instead, comparing the blue and mustard lines, we see that this parameter computed using our new parameterization presents overall agreement with respect to the full solution. In Ref. [86], it was found that a small viscosity, around $c_{\text{vis}}^2 \sim 10^{-4}$ for the w CDM model, could be detected by Euclid when weak lensing and galaxy clustering data are combined. Although in Ref. [86], the viscosity parameter was taken as a constant, which is not realistic in a general dark energy scenario as was pointed out in Ref. [58], if we take

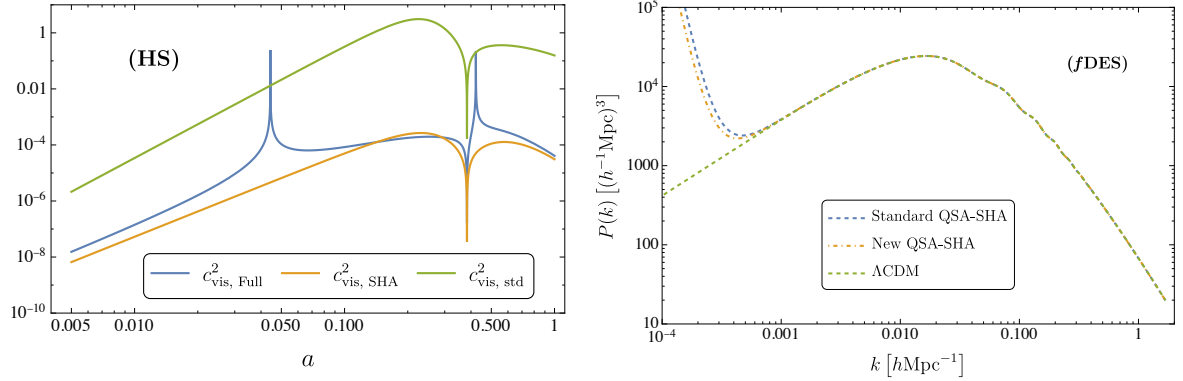


Figure 8. Left: Evolution of the viscosity parameter c_{vis}^2 for the HS model. We see that the evolution obtained using our new SHA parameterization (mustard line) agrees in overall with full numerical solution (blue line), while the result obtained from the standard QSA-SHA procedure (green line) gives a large over-estimation of this parameter. For the plot we took $k = 300H_0$. Right: Matter power spectrum for the f DES model using the standard procedure (blue dashed line) and the new parameterization (mustard dashed line). We also plot the Λ CDM result for comparison (green dashed line). We see that these results are completely indistinguishable for $k \gtrsim 0.001 h \text{Mpc}^{-1} \sim 3H_0$, while for smaller values of k both methods give divergent results, mainly due to that the SHA is not applicable.

this constant value as a representative value of the smallness of c_{vis}^2 , we see that our new parameterization indeed agrees with it.

7.2 The Matter Power Spectrum

In the right panel of Fig. 8 are depicted the linear matter power spectrum for the f DES model using the standard QSA-SHA procedure and our new approach. Also, the Λ CDM Planck best-fit 2018 standard result is shown for comparison. We can see in this plot that f DES is completely degenerate with respect to Λ CDM for modes $k \gtrsim 0.001 h \text{ Mpc}^{-1}$. For smaller modes, or equivalently for larger scales, both methods yield to divergent results.

As mentioned in previous sections, we do not expect the QSA and the SHA hold for modes smaller than $k < 200H_0 \sim 0.01 h \text{Mpc}^{-1}$. Moreover, note that in the region $k \lesssim k_{\text{eq}}$, where k_{eq} is the mode entering the horizon at the radiation-matter equilibrium, radiation is not negligible anymore. Therefore, the expansion history cannot be described using the Hubble parameter in Eq. (2.5) and the perturbations do not follow equations similar to Eqs. (2.6)-(2.9). As a comment, note that similar divergent results for the matter power spectrum were also found in Ref. [60] for Scalar-Vector-Tensor theories [90, 91].

We would like to mention that we also computed the CMB angular power spectrum using `EFCLASS`, and the $f\sigma_8$ function, for the models we are considering here. However, we do not find any appreciable difference between our results and those reported in Ref. [58]. Then, in order to keep our presentation simple, we do not show these results here, and rather we refer the reader to Figs. 5, 6, and 7 in Ref. [58]. Note that the similitude of the $f\sigma_8$ does not come as a surprise since both methods provide very similar result for the potentials Ψ and Φ ; as shown in Fig. 2, which yields to similar results for G_{eff} and Q_{eff} .

8 Conclusions

In this work, we have revisited the quasi-static and sub-horizon approximations when applied to $f(R)$ theories. We do so by proposing a parameterization using slow-rolling functions (like in inflation) which allowed us to track the relevance of time-derivatives of the gravitational potentials and the scale k in contrast to the expansion rate H [see Eqs. (4.1) and (4.2)]. In the effective fluid approach to $f(R)$, we showed that the standard QSA-SHA results found in the literature [Eqs. (3.22)-(3.26)] correspond to the 0 order expansion in our new parameterization. However, the neglected terms turned out to be significant for some of the dark energy effective fluid quantities. In particular, we found large differences in the DE scalar velocity V_{DE} and a minor correction in the sound speed $c_{s,\text{DE}}^2$. We then assessed the accuracy of our expressions [Eqs. (4.9)-(4.14)], and the standard QSA-SHA results, by comparing with results obtained from a full numerical solution of the linear perturbation equations. In Figs. 5, 6, and 8, we indeed corroborated that our expressions provide more accurate descriptions than the standard ones found in the literature.

Furthermore, we estimated a “safety region” where the QSA and the SHA can be applied. We found that the QSA and the second order expansion in the SHA yield very accurate results from matter domination $a \gtrsim 0.01$ to the present ($a = 1$) whenever $k \gtrsim 200H_0 \simeq 0.01 \text{ hMpc}^{-1}$. We also showed for a particular value out of this region that the time-derivatives of the potentials become important (see Fig. 7). This can also be seen in the matter power spectrum depicted in the right panel of Fig. 8, where we can see that the curves diverge for k small. We would like to stress that a similar divergent behavior was found in Ref. [60]. However, note that previous works on Horndeski theories [59], and Scalar-Vector-Tensor theories [60], where these approximations were used, all of them agree, in their corresponding limits, with the standard expressions in $f(R)$.

To conclude, clearly our results warrant performing a more in-depth analysis of the validity of the QSA and the SHA approximations in more generalized MG theories, e.g. of the Horndeski type, however we leave this for future work.

Numerical Codes: The codes used by the authors in the analysis of this paper will be made publicly available upon publication at <https://github.com/BayronO/QSA-SHA-for-Modified-Gravity>.

Acknowledgements

The authors are grateful to Rubén Arjona, Wilmar Cardona, and César Valenzuela-Toledo for useful discussions. BOQ would like to express his gratitude to the Instituto de Física Teórica UAM-CSIC, in Universidad Autónoma de Madrid, for the hospitality and kind support during early stages of this work. BOQ is also supported by Patrimonio Autónomo - Fondo Nacional de Financiamiento para la Ciencia, la Tecnología y la Innovación Francisco José de Caldas (MINCIENCIAS - COLOMBIA) Grant No. 110685269447 RC-80740-465- 2020, projects 69723 and 69553. SN acknowledges support from the research project PID2021-123012NB-C43, and the Spanish Research Agency (Agencia Estatal de Investigación) via the Grant IFT Centro de Excelencia Severo Ochoa No CEX2020-001007-S, funded by MCIN/AEI/10.13039/501100011033.

A Linear Field Equations in $f(R)$

Here we present the expressions for the coefficients in Eqs. (3.6)-(3.9):

$$A_1 = 3\dot{F} + 3FH, \quad A_2 = -3FH, \quad A_3 = 3F\dot{H} + 3FH^2 - 3H\dot{F}, \quad (A.1)$$

$$A_4 = F, \quad A_5 = 3F\dot{H} - 3FH^2 - 9H\dot{F}, \quad A_6 = -F.$$

$$C_1 = -F, \quad C_2 = F, \quad C_3 = \dot{F} - FH, \quad C_4 = 2\dot{F} + FH. \quad (A.2)$$

$$B_1 = 3F, \quad B_2 = -3F, \quad B_3 = 12FH, \quad B_4 = -12FH - 9\dot{F}, \quad (A.3)$$

$$B_5 = 3F\dot{H} + 9FH^2 - 6H\dot{F} - 3\ddot{F}, \quad B_6 = -9F\dot{H} - 9FH^2 - 18H\dot{F} - 9\ddot{F}.$$

$$D_1 = 3, \quad D_2 = 12H, \quad D_3 = -3H, \quad D_4 = \frac{F}{2F_R}, \quad (A.4)$$

$$D_5 = 2, \quad D_6 = \frac{F}{2F_R} - 6\dot{H} - 12H^2, \quad D_7 = 1.$$

B Dark Energy Perturbations in $f(R)$

Here we present the expressions for the coefficients in Eqs. (3.12)-(3.14):

$$W_1 = 6H - 3FH - 3\dot{F}, \quad W_2 = 3FH, \quad W_3 = -3F\dot{H} - 3FH^2 + 3H\dot{F}, \quad (B.1)$$

$$W_4 = 2 - F, \quad W_5 = 3H^2F - 6H^2 - 3F\dot{H} + 9H\dot{F}, \quad W_6 = F,$$

$$Y_1 = F - 2, \quad Y_2 = -F, \quad Y_3 = 4FH - 6H, \quad Y_4 = 2H - 4FH - 3\dot{F}, \quad (B.2)$$

$$Y_5 = 3FH^2 + F\dot{H} - 2H\dot{F} - \ddot{F}, \quad Y_6 = -\frac{2}{3},$$

$$Y_7 = 6H^2 - 3FH^2 + 4\dot{H} - 3F\dot{H} - 6H\dot{F} - 3\ddot{F}, \quad Y_8 = -\frac{2}{3},$$

$$Z_1 = F - 2, \quad Z_2 = -F, \quad Z_3 = FH - \dot{F}, \quad Z_4 = 2H - FH - 2\dot{F}. \quad (B.3)$$

C Linear Field Equations in the New Parameterization

Here we present the expressions for the coefficients in Eqs. (4.5)-(4.6):

$$\mathcal{A}_1 = -\mathcal{A}_4 = F, \quad \mathcal{A}_2 = 3F(\delta + \varepsilon_\Phi), \quad \mathcal{A}_3 = 18F_R(\varepsilon_\Phi - 1)(\delta + \xi - 2), \quad (C.1)$$

$$\mathcal{A}_5 = 3F(\delta - \varepsilon_\Psi - 2), \quad \mathcal{A}_6 = -54F_R(\delta + \xi - 2),$$

$$\mathcal{D}_1 = \mathcal{D}_4 = \frac{F}{2F_R}, \quad \mathcal{D}_2 = 2, \quad \mathcal{D}_3 = 3\varepsilon_\Phi(3 + \delta + \varepsilon_\Phi + \chi_\Phi), \quad (C.2)$$

$$\mathcal{D}_5 = 1, \quad \mathcal{D}_6 = -3(2 + 2\delta + \varepsilon_\Psi).$$

References

- [1] P. J. E. Peebles, *Cosmology's Century: An Inside History of Our Modern Understanding of the Universe*. Princeton University Press, 2020.
- [2] E. Di Valentino *et al.*, *Snowmass2021 - Letter of interest cosmology intertwined II: The hubble constant tension*, *Astropart. Phys.* **131** (2021) 102605, [[arXiv:2008.11284](https://arxiv.org/abs/2008.11284)], [[doi:10.1016/j.astropartphys.2021.102605](https://doi.org/10.1016/j.astropartphys.2021.102605)].
- [3] E. Di Valentino *et al.*, *Cosmology Intertwined III: $f\sigma_8$ and S_8* , *Astropart. Phys.* **131** (2021) 102604, [[arXiv:2008.11285](https://arxiv.org/abs/2008.11285)], [[doi:10.1016/j.astropartphys.2021.102604](https://doi.org/10.1016/j.astropartphys.2021.102604)].
- [4] E. Abdalla *et al.*, *Cosmology intertwined: A review of the particle physics, astrophysics, and cosmology associated with the cosmological tensions and anomalies*, *JHEAp* **34** (2022) 49–211, [[arXiv:2203.06142](https://arxiv.org/abs/2203.06142)], [[doi:10.1016/j.jheap.2022.04.002](https://doi.org/10.1016/j.jheap.2022.04.002)].
- [5] **Planck** Collaboration, N. Aghanim *et al.*, *Planck 2018 results. VI. Cosmological parameters*, *Astron. Astrophys.* **641** (2020) A6, [[arXiv:1807.06209](https://arxiv.org/abs/1807.06209)], [[doi:10.1051/0004-6361/201833910](https://doi.org/10.1051/0004-6361/201833910)]. [Erratum: *Astron. Astrophys.* 652, C4 (2021)].
- [6] A. G. Riess, S. Casertano, W. Yuan, L. M. Macri, and D. Scolnic, *Large Magellanic Cloud Cepheid Standards Provide a 1% Foundation for the Determination of the Hubble Constant and Stronger Evidence for Physics beyond Λ CDM*, *Astrophys. J.* **876** (2019), no. 1 85, [[arXiv:1903.07603](https://arxiv.org/abs/1903.07603)], [[doi:10.3847/1538-4357/ab1422](https://doi.org/10.3847/1538-4357/ab1422)].
- [7] A. G. Riess *et al.*, *A Comprehensive Measurement of the Local Value of the Hubble Constant with $1 \text{ km s}^{-1} \text{ Mpc}^{-1}$ Uncertainty from the Hubble Space Telescope and the SH0ES Team*, *Astrophys. J. Lett.* **934** (2022), no. 1 L7, [[arXiv:2112.04510](https://arxiv.org/abs/2112.04510)], [[doi:10.3847/2041-8213/ac5c5b](https://doi.org/10.3847/2041-8213/ac5c5b)].
- [8] K. C. Wong *et al.*, *H0LiCOW – XIII. A 2.4 per cent measurement of H_0 from lensed quasars: 5.3σ tension between early- and late-Universe probes*, *Mon. Not. Roy. Astron. Soc.* **498** (2020), no. 1 1420–1439, [[arXiv:1907.04869](https://arxiv.org/abs/1907.04869)], [[doi:10.1093/mnras/stz3094](https://doi.org/10.1093/mnras/stz3094)].
- [9] W. L. Freedman, *Measurements of the Hubble Constant: Tensions in Perspective*, *Astrophys. J.* **919** (2021), no. 1 16, [[arXiv:2106.15656](https://arxiv.org/abs/2106.15656)], [[doi:10.3847/1538-4357/ac0e95](https://doi.org/10.3847/1538-4357/ac0e95)].
- [10] **BOSS** Collaboration, S. Alam *et al.*, *The clustering of galaxies in the completed SDSS-III Baryon Oscillation Spectroscopic Survey: cosmological analysis of the DR12 galaxy sample*, *Mon. Not. Roy. Astron. Soc.* **470** (2017), no. 3 2617–2652, [[arXiv:1607.03155](https://arxiv.org/abs/1607.03155)], [[doi:10.1093/mnras/stx721](https://doi.org/10.1093/mnras/stx721)].
- [11] C. Heymans *et al.*, *KiDS-1000 Cosmology: Multi-probe weak gravitational lensing and spectroscopic galaxy clustering constraints*, *Astron. Astrophys.* **646** (2021) A140, [[arXiv:2007.15632](https://arxiv.org/abs/2007.15632)], [[doi:10.1051/0004-6361/202039063](https://doi.org/10.1051/0004-6361/202039063)].
- [12] **KiDS, Euclid** Collaboration, A. Loureiro *et al.*, *KiDS and Euclid: Cosmological implications of a pseudo angular power spectrum analysis of KiDS-1000 cosmic shear tomography*, *Astron. Astrophys.* **665** (2022) A56, [[arXiv:2110.06947](https://arxiv.org/abs/2110.06947)], [[doi:10.1051/0004-6361/202142481](https://doi.org/10.1051/0004-6361/202142481)].
- [13] **DES, SPT** Collaboration, C. Chang *et al.*, *Joint analysis of Dark Energy Survey Year 3 data and CMB lensing from SPT and Planck. II. Cross-correlation measurements and cosmological constraints*, *Phys. Rev. D* **107** (2023), no. 2 023530, [[arXiv:2203.12440](https://arxiv.org/abs/2203.12440)], [[doi:10.1103/PhysRevD.107.023530](https://doi.org/10.1103/PhysRevD.107.023530)].
- [14] E. Macaulay, I. K. Wehus, and H. K. Eriksen, *Lower Growth Rate from Recent Redshift Space Distortion Measurements than Expected from Planck*, *Phys. Rev. Lett.* **111** (2013), no. 16 161301, [[arXiv:1303.6583](https://arxiv.org/abs/1303.6583)], [[doi:10.1103/PhysRevLett.111.161301](https://doi.org/10.1103/PhysRevLett.111.161301)].
- [15] R. A. Battye, T. Charnock, and A. Moss, *Tension between the power spectrum of density perturbations measured on large and small scales*, *Phys. Rev. D* **91** (2015), no. 10 103508, [[arXiv:1409.2769](https://arxiv.org/abs/1409.2769)], [[doi:10.1103/PhysRevD.91.103508](https://doi.org/10.1103/PhysRevD.91.103508)].

[16] M. Ata *et al.*, *The clustering of the SDSS-IV extended Baryon Oscillation Spectroscopic Survey DR14 quasar sample: first measurement of baryon acoustic oscillations between redshift 0.8 and 2.2*, *Mon. Not. Roy. Astron. Soc.* **473** (2018), no. 4 4773–4794, [[arXiv:1705.06373](https://arxiv.org/abs/1705.06373)], [[doi:10.1093/mnras/stx2630](https://doi.org/10.1093/mnras/stx2630)].

[17] O. H. E. Philcox and M. M. Ivanov, *BOSS DR12 full-shape cosmology: Λ CDM constraints from the large-scale galaxy power spectrum and bispectrum monopole*, *Phys. Rev. D* **105** (2022), no. 4 043517, [[arXiv:2112.04515](https://arxiv.org/abs/2112.04515)], [[doi:10.1103/PhysRevD.105.043517](https://doi.org/10.1103/PhysRevD.105.043517)].

[18] Y. Kobayashi, T. Nishimichi, M. Takada, and H. Miyatake, *Full-shape cosmology analysis of the SDSS-III BOSS galaxy power spectrum using an emulator-based halo model: A 5% determination of σ_8* , *Phys. Rev. D* **105** (2022), no. 8 083517, [[arXiv:2110.06969](https://arxiv.org/abs/2110.06969)], [[doi:10.1103/PhysRevD.105.083517](https://doi.org/10.1103/PhysRevD.105.083517)].

[19] L. Huang, Z. Huang, H. Zhou, and Z. Li, *The S_8 tension in light of updated redshift-space distortion data and PAge approximation*, *Sci. China Phys. Mech. Astron.* **65** (2022), no. 3 239512, [[arXiv:2110.08498](https://arxiv.org/abs/2110.08498)], [[doi:10.1007/s11433-021-1838-1](https://doi.org/10.1007/s11433-021-1838-1)].

[20] A. Blanchard and S. Ilić, *Closing up the cluster tension?*, *Astron. Astrophys.* **656** (2021) A75, [[arXiv:2104.00756](https://arxiv.org/abs/2104.00756)], [[doi:10.1051/0004-6361/202140974](https://doi.org/10.1051/0004-6361/202140974)].

[21] N. J. Secrest, S. von Hausegger, M. Rameez, R. Mohayaee, S. Sarkar, and J. Colin, *A Test of the Cosmological Principle with Quasars*, *Astrophys. J. Lett.* **908** (2021), no. 2 L51, [[arXiv:2009.14826](https://arxiv.org/abs/2009.14826)], [[doi:10.3847/2041-8213/abdd40](https://doi.org/10.3847/2041-8213/abdd40)].

[22] C. Dalang and C. Bonvin, *On the kinematic cosmic dipole tension*, *Mon. Not. Roy. Astron. Soc.* **512** (2022), no. 3 3895–3905, [[arXiv:2111.03616](https://arxiv.org/abs/2111.03616)], [[doi:10.1093/mnras/stac726](https://doi.org/10.1093/mnras/stac726)].

[23] N. J. Secrest, S. von Hausegger, M. Rameez, R. Mohayaee, and S. Sarkar, *A Challenge to the Standard Cosmological Model*, *Astrophys. J. Lett.* **937** (2022), no. 2 L31, [[arXiv:2206.05624](https://arxiv.org/abs/2206.05624)], [[doi:10.3847/2041-8213/ac88c0](https://doi.org/10.3847/2041-8213/ac88c0)].

[24] L. Dam, G. F. Lewis, and B. J. Brewer, *Testing the Cosmological Principle with CatWISE Quasars: A Bayesian Analysis of the Number-Count Dipole*, [arXiv:2212.07733](https://arxiv.org/abs/2212.07733).

[25] B. D. Fields, *The primordial lithium problem*, *Ann. Rev. Nucl. Part. Sci.* **61** (2011) 47–68, [[arXiv:1203.3551](https://arxiv.org/abs/1203.3551)], [[doi:10.1146/annurev-nucl-102010-130445](https://doi.org/10.1146/annurev-nucl-102010-130445)].

[26] R. H. Cyburt, B. D. Fields, K. A. Olive, and T.-H. Yeh, *Big Bang Nucleosynthesis: 2015*, *Rev. Mod. Phys.* **88** (2016) 015004, [[arXiv:1505.01076](https://arxiv.org/abs/1505.01076)], [[doi:10.1103/RevModPhys.88.015004](https://doi.org/10.1103/RevModPhys.88.015004)].

[27] C. Pitrou, A. Coc, J.-P. Uzan, and E. Vangioni, *A new tension in the cosmological model from primordial deuterium?*, *Mon. Not. Roy. Astron. Soc.* **502** (2021), no. 2 2474–2481, [[arXiv:2011.11320](https://arxiv.org/abs/2011.11320)], [[doi:10.1093/mnras/stab135](https://doi.org/10.1093/mnras/stab135)].

[28] L. Perivolaropoulos and F. Skara, *Challenges for Λ CDM: An update*, *New Astron. Rev.* **95** (2022) 101659, [[arXiv:2105.05208](https://arxiv.org/abs/2105.05208)], [[doi:10.1016/j.newar.2022.101659](https://doi.org/10.1016/j.newar.2022.101659)].

[29] **Euclid** Collaboration, S. Nesseris *et al.*, *Euclid: Forecast constraints on consistency tests of the Λ CDM model*, *Astron. Astrophys.* **660** (2022) A67, [[arXiv:2110.11421](https://arxiv.org/abs/2110.11421)], [[doi:10.1051/0004-6361/202142503](https://doi.org/10.1051/0004-6361/202142503)].

[30] **Euclid** Collaboration, D. Camarena *et al.*, *Euclid: Testing the Copernican principle with next-generation surveys*, [arXiv:2207.09995](https://arxiv.org/abs/2207.09995), [doi:10.1051/0004-6361/202244557](https://doi.org/10.1051/0004-6361/202244557).

[31] L. Perivolaropoulos, *Large Scale Cosmological Anomalies and Inhomogeneous Dark Energy*, *Galaxies* **2** (2014) 22–61, [[arXiv:1401.5044](https://arxiv.org/abs/1401.5044)], [[doi:10.3390/galaxies2010022](https://doi.org/10.3390/galaxies2010022)].

[32] J. Garcia-Bellido and T. Haugboelle, *Confronting Lemaitre-Tolman-Bondi models with Observational Cosmology*, *JCAP* **04** (2008) 003, [[arXiv:0802.1523](https://arxiv.org/abs/0802.1523)], [[doi:10.1088/1475-7516/2008/04/003](https://doi.org/10.1088/1475-7516/2008/04/003)].

[33] J. Garcia-Bellido and T. Haugboelle, *Looking the void in the eyes - the kSZ effect in LTB models*, *JCAP* **09** (2008) 016, [[arXiv:0807.1326](https://arxiv.org/abs/0807.1326)], [[doi:10.1088/1475-7516/2008/09/016](https://doi.org/10.1088/1475-7516/2008/09/016)].

[34] M. Redlich, K. Bolejko, S. Meyer, G. F. Lewis, and M. Bartelmann, *Probing spatial homogeneity with LTB models: a detailed discussion*, *Astron. Astrophys.* **570** (2014) A63, [[arXiv:1408.1872](https://arxiv.org/abs/1408.1872)], [[doi:10.1051/0004-6361/201424553](https://doi.org/10.1051/0004-6361/201424553)].

[35] J. B. Orjuela-Quintana, M. Alvarez, C. A. Valenzuela-Toledo, and Y. Rodriguez, *Anisotropic Einstein Yang-Mills Higgs Dark Energy*, *JCAP* **10** (2020) 019, [[arXiv:2006.14016](https://arxiv.org/abs/2006.14016)], [[doi:10.1088/1475-7516/2020/10/019](https://doi.org/10.1088/1475-7516/2020/10/019)].

[36] A. Guarnizo, J. B. Orjuela-Quintana, and C. A. Valenzuela-Toledo, *Dynamical analysis of cosmological models with non-Abelian gauge vector fields*, *Phys. Rev. D* **102** (2020), no. 083507, [[arXiv:2007.12964](https://arxiv.org/abs/2007.12964)], [[doi:10.1103/PhysRevD.102.083507](https://doi.org/10.1103/PhysRevD.102.083507)].

[37] J. Motoa-Manzano, J. Bayron Orjuela-Quintana, T. S. Pereira, and C. A. Valenzuela-Toledo, *Anisotropic solid dark energy*, *Phys. Dark Univ.* **32** (2021) 100806, [[arXiv:2012.09946](https://arxiv.org/abs/2012.09946)], [[doi:10.1016/j.dark.2021.100806](https://doi.org/10.1016/j.dark.2021.100806)].

[38] J. B. Orjuela-Quintana and C. A. Valenzuela-Toledo, *Anisotropic k-essence*, *Phys. Dark Univ.* **33** (2021) 100857, [[arXiv:2106.06432](https://arxiv.org/abs/2106.06432)], [[doi:10.1016/j.dark.2021.100857](https://doi.org/10.1016/j.dark.2021.100857)].

[39] J. P. Beltrán Almeida, J. Motoa-Manzano, J. Noreña, T. S. Pereira, and C. A. Valenzuela-Toledo, *Structure formation in an anisotropic universe: Eulerian perturbation theory*, *JCAP* **02** (2022), no. 02 018, [[arXiv:2111.06756](https://arxiv.org/abs/2111.06756)], [[doi:10.1088/1475-7516/2022/02/018](https://doi.org/10.1088/1475-7516/2022/02/018)].

[40] E. J. Copeland, M. Sami, and S. Tsujikawa, *Dynamics of dark energy*, *Int. J. Mod. Phys. D* **15** (2006) 1753–1936, [[arXiv:hep-th/0603057](https://arxiv.org/abs/hep-th/0603057)], [[doi:10.1142/S021827180600942X](https://doi.org/10.1142/S021827180600942X)].

[41] L. Amendola and S. Tsujikawa, *Dark Energy: Theory and Observations*. Cambridge University Press, 1, 2015.

[42] T. Clifton, P. G. Ferreira, A. Padilla, and C. Skordis, *Modified Gravity and Cosmology*, *Phys. Rept.* **513** (2012) 1–189, [[arXiv:1106.2476](https://arxiv.org/abs/1106.2476)], [[doi:10.1016/j.physrep.2012.01.001](https://doi.org/10.1016/j.physrep.2012.01.001)].

[43] **CANTATA** Collaboration, E. N. Saridakis et al., *Modified Gravity and Cosmology: An Update by the CANTATA Network*, [arXiv:2105.12582](https://arxiv.org/abs/2105.12582).

[44] **LIGO Scientific, Virgo** Collaboration, B. P. Abbott et al., *GW170814: A Three-Detector Observation of Gravitational Waves from a Binary Black Hole Coalescence*, *Phys. Rev. Lett.* **119** (2017), no. 14 141101, [[arXiv:1709.09660](https://arxiv.org/abs/1709.09660)], [[doi:10.1103/PhysRevLett.119.141101](https://doi.org/10.1103/PhysRevLett.119.141101)].

[45] J. M. Ezquiaga and M. Zumalacárregui, *Dark Energy After GW170817: Dead Ends and the Road Ahead*, *Phys. Rev. Lett.* **119** (2017), no. 25 251304, [[arXiv:1710.05901](https://arxiv.org/abs/1710.05901)], [[doi:10.1103/PhysRevLett.119.251304](https://doi.org/10.1103/PhysRevLett.119.251304)].

[46] **Planck** Collaboration, P. A. R. Ade et al., *Planck 2015 results. XIV. Dark energy and modified gravity*, *Astron. Astrophys.* **594** (2016) A14, [[arXiv:1502.01590](https://arxiv.org/abs/1502.01590)], [[doi:10.1051/0004-6361/201525814](https://doi.org/10.1051/0004-6361/201525814)].

[47] **LIGO Scientific, Virgo** Collaboration, B. P. Abbott et al., *Tests of general relativity with GW150914*, *Phys. Rev. Lett.* **116** (2016), no. 22 221101, [[arXiv:1602.03841](https://arxiv.org/abs/1602.03841)], [[doi:10.1103/PhysRevLett.116.221101](https://doi.org/10.1103/PhysRevLett.116.221101)]. [Erratum: *Phys. Rev. Lett.* 121, 129902 (2018)].

[48] T. E. Collett, L. J. Oldham, R. J. Smith, M. W. Auger, K. B. Westfall, D. Bacon, R. C. Nichol, K. L. Masters, K. Koyama, and R. van den Bosch, *A precise extragalactic test of General Relativity*, *Science* **360** (2018) 1342, [[arXiv:1806.08300](https://arxiv.org/abs/1806.08300)], [[doi:10.1126/science.aoa2469](https://doi.org/10.1126/science.aoa2469)].

[49] A. De Felice and S. Tsujikawa, *f(R) theories*, *Living Rev. Rel.* **13** (2010) 3, [[arXiv:1002.4928](https://arxiv.org/abs/1002.4928)], [[doi:10.12942/lrr-2010-3](https://doi.org/10.12942/lrr-2010-3)].

[50] L. Pogosian and A. Silvestri, *The pattern of growth in viable f(R) cosmologies*, *Phys. Rev. D* **77**

(2008) 023503, [[arXiv:0709.0296](https://arxiv.org/abs/0709.0296)], [[doi:10.1103/PhysRevD.77.023503](https://doi.org/10.1103/PhysRevD.77.023503)]. [Erratum: Phys. Rev. D 81, 049901 (2010)].

[51] J. Pérez-Romero and S. Nesseris, *Cosmological constraints and comparison of viable $f(R)$ models*, Phys. Rev. D **97** (2018), no. 2 023525, [[arXiv:1710.05634](https://arxiv.org/abs/1710.05634)], [[doi:10.1103/PhysRevD.97.023525](https://doi.org/10.1103/PhysRevD.97.023525)].

[52] C. Álvarez Luna, S. Basilakos, and S. Nesseris, *Cosmological constraints on γ -gravity models*, Phys. Rev. D **98** (2018), no. 2 023516, [[arXiv:1805.02926](https://arxiv.org/abs/1805.02926)], [[doi:10.1103/PhysRevD.98.023516](https://doi.org/10.1103/PhysRevD.98.023516)].

[53] S. Nesseris, *The Effective Fluid approach for Modified Gravity and its applications*, Universe **9** (2023) 2022, [[arXiv:2212.12768](https://arxiv.org/abs/2212.12768)], [[doi:10.3390/universe9010013](https://doi.org/10.3390/universe9010013)].

[54] G. Gubitosi, F. Piazza, and F. Vernizzi, *The Effective Field Theory of Dark Energy*, JCAP **02** (2013) 032, [[arXiv:1210.0201](https://arxiv.org/abs/1210.0201)], [[doi:10.1088/1475-7516/2013/02/032](https://doi.org/10.1088/1475-7516/2013/02/032)].

[55] J. K. Bloomfield, E. E. Flanagan, M. Park, and S. Watson, *Dark energy or modified gravity? An effective field theory approach*, JCAP **08** (2013) 010, [[arXiv:1211.7054](https://arxiv.org/abs/1211.7054)], [[doi:10.1088/1475-7516/2013/08/010](https://doi.org/10.1088/1475-7516/2013/08/010)].

[56] B. Hu, M. Raveri, N. Frusciante, and A. Silvestri, *Effective Field Theory of Cosmic Acceleration: an implementation in CAMB*, Phys. Rev. D **89** (2014), no. 10 103530, [[arXiv:1312.5742](https://arxiv.org/abs/1312.5742)], [[doi:10.1103/PhysRevD.89.103530](https://doi.org/10.1103/PhysRevD.89.103530)].

[57] N. Frusciante and L. Perenon, *Effective field theory of dark energy: A review*, Phys. Rept. **857** (2020) 1–63, [[arXiv:1907.03150](https://arxiv.org/abs/1907.03150)], [[doi:10.1016/j.physrep.2020.02.004](https://doi.org/10.1016/j.physrep.2020.02.004)].

[58] R. Arjona, W. Cardona, and S. Nesseris, *Unraveling the effective fluid approach for $f(R)$ models in the subhorizon approximation*, Phys. Rev. D **99** (2019), no. 4 043516, [[arXiv:1811.02469](https://arxiv.org/abs/1811.02469)], [[doi:10.1103/PhysRevD.99.043516](https://doi.org/10.1103/PhysRevD.99.043516)].

[59] R. Arjona, W. Cardona, and S. Nesseris, *Designing Horndeski and the effective fluid approach*, Phys. Rev. D **100** (2019), no. 6 063526, [[arXiv:1904.06294](https://arxiv.org/abs/1904.06294)], [[doi:10.1103/PhysRevD.100.063526](https://doi.org/10.1103/PhysRevD.100.063526)].

[60] W. Cardona, J. B. Orjuela-Quintana, and C. A. Valenzuela-Toledo, *An effective fluid description of scalar-vector-tensor theories under the sub-horizon and quasi-static approximations*, JCAP **08** (2022), no. 08 059, [[arXiv:2206.02895](https://arxiv.org/abs/2206.02895)], [[doi:10.1088/1475-7516/2022/08/059](https://doi.org/10.1088/1475-7516/2022/08/059)].

[61] D. Blas, J. Lesgourges, and T. Tram, *The Cosmic Linear Anisotropy Solving System (CLASS) II: Approximation schemes*, JCAP **1107** (2011) 034, [[arXiv:1104.2933](https://arxiv.org/abs/1104.2933)], [[doi:10.1088/1475-7516/2011/07/034](https://doi.org/10.1088/1475-7516/2011/07/034)].

[62] S. Tsujikawa, *Matter density perturbations and effective gravitational constant in modified gravity models of dark energy*, Phys. Rev. D **76** (2007) 023514, [[arXiv:0705.1032](https://arxiv.org/abs/0705.1032)], [[doi:10.1103/PhysRevD.76.023514](https://doi.org/10.1103/PhysRevD.76.023514)].

[63] J. Noller, F. von Braun-Bates, and P. G. Ferreira, *Relativistic scalar fields and the quasistatic approximation in theories of modified gravity*, Phys. Rev. D **89** (2014), no. 2 023521, [[arXiv:1310.3266](https://arxiv.org/abs/1310.3266)], [[doi:10.1103/PhysRevD.89.023521](https://doi.org/10.1103/PhysRevD.89.023521)].

[64] A. Silvestri, L. Pogosian, and R. V. Buniy, *Practical approach to cosmological perturbations in modified gravity*, Phys. Rev. D **87** (2013), no. 10 104015, [[arXiv:1302.1193](https://arxiv.org/abs/1302.1193)], [[doi:10.1103/PhysRevD.87.104015](https://doi.org/10.1103/PhysRevD.87.104015)].

[65] S. Bose, W. A. Hellwing, and B. Li, *Testing the quasi-static approximation in $f(R)$ gravity simulations*, JCAP **02** (2015) 034, [[arXiv:1411.6128](https://arxiv.org/abs/1411.6128)], [[doi:10.1088/1475-7516/2015/02/034](https://doi.org/10.1088/1475-7516/2015/02/034)].

[66] E. Bellini and I. Sawicki, *Maximal freedom at minimum cost: linear large-scale structure in general modifications of gravity*, JCAP **07** (2014) 050, [[arXiv:1404.3713](https://arxiv.org/abs/1404.3713)], [[doi:10.1088/1475-7516/2014/07/050](https://doi.org/10.1088/1475-7516/2014/07/050)].

[67] J. Gleyzes, D. Langlois, and F. Vernizzi, *A unifying description of dark energy*, *Int. J. Mod. Phys. D* **23** (2015), no. 13 1443010, [[arXiv:1411.3712](https://arxiv.org/abs/1411.3712)], [[doi:10.1142/S021827181443010X](https://doi.org/10.1142/S021827181443010X)].

[68] I. Sawicki and E. Bellini, *Limits of quasistatic approximation in modified-gravity cosmologies*, *Phys. Rev. D* **92** (2015), no. 8 084061, [[arXiv:1503.06831](https://arxiv.org/abs/1503.06831)], [[doi:10.1103/PhysRevD.92.084061](https://doi.org/10.1103/PhysRevD.92.084061)].

[69] L. Pogosian and A. Silvestri, *What can cosmology tell us about gravity? Constraining Horndeski gravity with Σ and μ* , *Phys. Rev. D* **94** (2016), no. 10 104014, [[arXiv:1606.05339](https://arxiv.org/abs/1606.05339)], [[doi:10.1103/PhysRevD.94.104014](https://doi.org/10.1103/PhysRevD.94.104014)].

[70] A. De Felice, L. Heisenberg, R. Kase, S. Mukohyama, S. Tsujikawa, and Y.-l. Zhang, *Effective gravitational couplings for cosmological perturbations in generalized Proca theories*, *Phys. Rev. D* **94** (2016), no. 4 044024, [[arXiv:1605.05066](https://arxiv.org/abs/1605.05066)], [[doi:10.1103/PhysRevD.94.044024](https://doi.org/10.1103/PhysRevD.94.044024)].

[71] F. Pace, R. Battye, E. Bellini, L. Lombriser, F. Vernizzi, and B. Bolliet, *Comparison of different approaches to the quasi-static approximation in Horndeski models*, *JCAP* **06** (2021) 017, [[arXiv:2011.05713](https://arxiv.org/abs/2011.05713)], [[doi:10.1088/1475-7516/2021/06/017](https://doi.org/10.1088/1475-7516/2021/06/017)].

[72] A. de la Cruz-Dombriz, A. Dobado, and A. L. Maroto, *On the evolution of density perturbations in $f(R)$ theories of gravity*, *Phys. Rev. D* **77** (2008) 123515, [[arXiv:0802.2999](https://arxiv.org/abs/0802.2999)], [[doi:10.1103/PhysRevD.77.123515](https://doi.org/10.1103/PhysRevD.77.123515)].

[73] C. Llinares and D. F. Mota, *Cosmological simulations of screened modified gravity out of the static approximation: effects on matter distribution*, *Phys. Rev. D* **89** (2014), no. 8 084023, [[arXiv:1312.6016](https://arxiv.org/abs/1312.6016)], [[doi:10.1103/PhysRevD.89.084023](https://doi.org/10.1103/PhysRevD.89.084023)].

[74] T. Multamaki and I. Vilja, *Cosmological expansion and the uniqueness of gravitational action*, *Phys. Rev. D* **73** (2006) 024018, [[arXiv:astro-ph/0506692](https://arxiv.org/abs/astro-ph/0506692)], [[doi:10.1103/PhysRevD.73.024018](https://doi.org/10.1103/PhysRevD.73.024018)].

[75] A. de la Cruz-Dombriz and A. Dobado, *A $f(R)$ gravity without cosmological constant*, *Phys. Rev. D* **74** (2006) 087501, [[arXiv:gr-qc/0607118](https://arxiv.org/abs/gr-qc/0607118)], [[doi:10.1103/PhysRevD.74.087501](https://doi.org/10.1103/PhysRevD.74.087501)].

[76] W. Hu and I. Sawicki, *A Parameterized Post-Friedmann Framework for Modified Gravity*, *Phys. Rev. D* **76** (2007) 104043, [[arXiv:0708.1190](https://arxiv.org/abs/0708.1190)], [[doi:10.1103/PhysRevD.76.104043](https://doi.org/10.1103/PhysRevD.76.104043)].

[77] S. Capozziello, V. F. Cardone, and A. Troisi, *Reconciling dark energy models with $f(R)$ theories*, *Phys. Rev. D* **71** (2005) 043503, [[arXiv:astro-ph/0501426](https://arxiv.org/abs/astro-ph/0501426)], [[doi:10.1103/PhysRevD.71.043503](https://doi.org/10.1103/PhysRevD.71.043503)].

[78] S. Nojiri and S. D. Odintsov, *Modified $f(R)$ gravity consistent with realistic cosmology: From matter dominated epoch to dark energy universe*, *Phys. Rev. D* **74** (2006) 086005, [[arXiv:hep-th/0608008](https://arxiv.org/abs/hep-th/0608008)], [[doi:10.1103/PhysRevD.74.086005](https://doi.org/10.1103/PhysRevD.74.086005)].

[79] S. Basilakos, S. Nesseris, and L. Perivolaropoulos, *Observational constraints on viable $f(R)$ parametrizations with geometrical and dynamical probes*, *Phys. Rev. D* **87** (2013), no. 12 123529, [[arXiv:1302.6051](https://arxiv.org/abs/1302.6051)], [[doi:10.1103/PhysRevD.87.123529](https://doi.org/10.1103/PhysRevD.87.123529)].

[80] SDSS Collaboration, M. Tegmark et al., *The 3-D power spectrum of galaxies from the SDSS*, *Astrophys. J.* **606** (2004) 702–740, [[arXiv:astro-ph/0310725](https://arxiv.org/abs/astro-ph/0310725)], [[doi:10.1086/382125](https://doi.org/10.1086/382125)].

[81] L. Amendola, R. Gannouji, D. Polarski, and S. Tsujikawa, *Conditions for the cosmological viability of $f(R)$ dark energy models*, *Phys. Rev. D* **75** (2007) 083504, [[arXiv:gr-qc/0612180](https://arxiv.org/abs/gr-qc/0612180)], [[doi:10.1103/PhysRevD.75.083504](https://doi.org/10.1103/PhysRevD.75.083504)].

[82] R. A. Battye, B. Bolliet, and F. Pace, *Do cosmological data rule out $f(\mathcal{R})$ with $w \neq -1$?*, *Phys. Rev. D* **97** (2018), no. 10 104070, [[arXiv:1712.05976](https://arxiv.org/abs/1712.05976)], [[doi:10.1103/PhysRevD.97.104070](https://doi.org/10.1103/PhysRevD.97.104070)].

[83] D. Sapone and M. Kunz, *Fingerprinting Dark Energy*, *Phys. Rev. D* **80** (2009) 083519, [[arXiv:0909.0007](https://arxiv.org/abs/0909.0007)], [[doi:10.1103/PhysRevD.80.083519](https://doi.org/10.1103/PhysRevD.80.083519)].

[84] A. A. Starobinsky, *Disappearing cosmological constant in $f(R)$ gravity*, *JETP Lett.* **86** (2007) 157–163, [[arXiv:0706.2041](https://arxiv.org/abs/0706.2041)], [[doi:10.1134/S0021364007150027](https://doi.org/10.1134/S0021364007150027)].

[85] W. Cardona, L. Hollenstein, and M. Kunz, *The traces of anisotropic dark energy in light of Planck*, *JCAP* **07** (2014) 032, [[arXiv:1402.5993](https://arxiv.org/abs/1402.5993)], [[doi:10.1088/1475-7516/2014/07/032](https://doi.org/10.1088/1475-7516/2014/07/032)].

- [86] D. Sapone, E. Majerotto, M. Kunz, and B. Garilli, *Can dark energy viscosity be detected with the Euclid survey?*, *Phys. Rev. D* **88** (2013) 043503, [[arXiv:1305.1942](https://arxiv.org/abs/1305.1942)], [[doi:10.1103/PhysRevD.88.043503](https://doi.org/10.1103/PhysRevD.88.043503)].
- [87] M. Kunz, *The phenomenological approach to modeling the dark energy*, *Comptes Rendus Physique* **13** (2012) 539–565, [[arXiv:1204.5482](https://arxiv.org/abs/1204.5482)], [[doi:10.1016/j.crhy.2012.04.007](https://doi.org/10.1016/j.crhy.2012.04.007)].
- [88] I. D. Saltas and M. Kunz, *Anisotropic stress and stability in modified gravity models*, *Phys. Rev. D* **83** (2011) 064042, [[arXiv:1012.3171](https://arxiv.org/abs/1012.3171)], [[doi:10.1103/PhysRevD.83.064042](https://doi.org/10.1103/PhysRevD.83.064042)].
- [89] W. Hu, *Structure formation with generalized dark matter*, *Astrophys. J.* **506** (1998) 485–494, [[arXiv:astro-ph/9801234](https://arxiv.org/abs/astro-ph/9801234)], [[doi:10.1086/306274](https://doi.org/10.1086/306274)].
- [90] L. Heisenberg, *Scalar-Vector-Tensor Gravity Theories*, *JCAP* **10** (2018) 054, [[arXiv:1801.01523](https://arxiv.org/abs/1801.01523)], [[doi:10.1088/1475-7516/2018/10/054](https://doi.org/10.1088/1475-7516/2018/10/054)].
- [91] L. Heisenberg, R. Kase, and S. Tsujikawa, *Cosmology in scalar-vector-tensor theories*, *Phys. Rev. D* **98** (2018), no. 2 024038, [[arXiv:1805.01066](https://arxiv.org/abs/1805.01066)], [[doi:10.1103/PhysRevD.98.024038](https://doi.org/10.1103/PhysRevD.98.024038)].